RADIONUCLIDE SORPTION IN FRACTURES AT YUCCA MOUNTAIN, NEVADA: A PRELIMINARY DEMONSTRATION OF APPROACH FOR PERFORMANCE ASSESSMENT

Prepared for

Nuclear Regulatory Commission
Contract NRC-02-97-009

Prepared by

David R. Turner

Center for Nuclear Waste Regulatory Analyses
San Antonio, Texas

April 1998

ABSTRACT

One of the Key Technical Issues (KTIs) identified by the Nuclear Regulatory Commission is focused on processes that control potential radionuclide transport from the proposed high-level radioactive waste repository at Yucca Mountain (YM), Nevada, through the natural barriers of the geological setting. One of these processes is the sorption of radionuclides onto minerals in the fractures. In contrast to the constant sorption coefficients (K_D) assumed in performance assessment (PA) models, sorption is controlled by water chemistry, and to a certain extent by the mineralogy and mineral surface area exposed in the fracture. In this report, an initial approach is developed to incorporate into PA calculations aspects of more detailed models that take into account the geochemical dependence of radionuclide sorption. The chemistry of saturated zone groundwater from the vicinity of YM, and the observed ranges of key measured parameters such as pH and total inorganic carbon that will exert control on radionuclide sorption behavior, are discussed. A key assumption is that the distribution of these parameters is representative of the range in water chemistries that is to be expected in the fracture system at YM. Geochemical speciation models are used to calculate site-specific distributions for additional parameters that may affect radionuclide transport such as ionic strength, PCO_2, and saturation indices for different minerals.

To obtain a mechanistic basis for sorption behavior for PA, a diffuse-layer surface complexation model is applied to calculate Np(V) and U(VI) sorption on montmorillonite for each water analysis; the resulting predicted sorption parameters are normalized to effective mineral surface area ($K_{A'}$). The population statistics for the distributions of these calculated sorption parameters indirectly represent the effects of site-specific geochemistry on potential radionuclide sorption, and can be used to constrain distributions that are currently used in PA. Because Np(V) and U(VI) sorption behavior as a function of geochemistry is similar for different types of aluminosilicates, the effective mineral surface area can then be used as a scaling factor to convert $K_{A'}$ to K_D for use in PA transport calculations. The Np(V) and U(VI) parameter distributions are calculated using the same water chemistries. This offers a means of estimating correlation among sorption parameters for different radionuclides, and uses site-specific water chemistry to link sorption parameter probability distribution functions in PA transport models.

CONTENTS

FIGURES

FIGURES (cont'd)

TABLES

ACKNOWLEDGMENTS

This report was prepared to document work performed by the Center for Nuclear Waste Regulatory Analyses (CNWRA) for the Nuclear Regulatory Commission (NRC) under Contract No. NRC-02-97-009. The activities reported here were performed on behalf of the NRC Office of Nuclear Material Safety and Safeguards (NMSS), Division of Waste Management (DWM). The report is an independent product of the CNWRA and does not necessarily reflect the views or regulatory position of the NRC.

QUALITY OF DATA, ANALYSES, AND CODE DEVELOPMENT

DATA: CNWRA-generated original data contained in this report meet quality assurance requirements described in the CNWRA Quality Assurance Manual. Sources for other data should be consulted for determining the level of quality for those data.

ANALYSES AND CODES: The MINTEQA2, Version 3.11 computer code was used for analyses contained in this report. This computer code is controlled under the CNWRA Software Configuration Procedures. The spreadsheet software Microsoft Excel, Version 5.0, was used in calculations and graphing of results presented in this report. This is a commercial spreadsheet software package and only the object code is available to the CNWRA.

1 INTRODUCTION

1.1 REGULATORY BACKGROUND

One of the primary objectives of the Nuclear Regulatory Commission (NRC) refocused prelicensing program is to direct its activities towards resolving the 10 key technical issues (KTIs) it considers most important to performance of the proposed high-level nuclear waste (HLW) repository at Yucca Mountain (YM). One of these KTIs is concerned with assessing the potential for radionuclide transport (RT) from the repository through the subsurface to the accessible environment.

A number of processes, such as sorption, matrix diffusion, dispersion, mineral precipitation, radioactive decay, and dilution may serve to retard RT and reduce dissolved radionuclide concentrations, ultimately leading to a reduction in potential dose to humans. In the July 1996 DOE Waste Containment and Isolation Strategy (WCIS) (U.S. Department of Energy, 1996) and the January 1998 Repository Safety Strategy (RSS) (U.S. Department of Energy, 1998), reduction in radionuclide concentrations during RT is mentioned as a key attribute that needs to be demonstrated in any suitability evaluation of a proposed repository at YM. Specifically, chemical properties of the system barriers (natural and engineered) that may operate to reduce radionuclide concentrations during transport (RSS— Hypothesis 14) need to be examined and evaluated. This need to consider retardation processes is especially true for time periods greater than 10,000 yr recommended for consideration by the National Academy of Science (National Research Council, 1995). The likely means that will be used to address this issue involve quantitative conceptual and numerical models in repository performance assessments (PA) describing RT under geochemical and hydrologic conditions specific to YM. Understanding geochemical processes that influence RT may be used to compensate for uncertainties in hydrologic models of the YM system (Simmons et al., 1995). Understanding the degree to which these processes are affected by changes in system chemistry/hydrology will help to reasonably bound rates of RT and reductions in radionuclide concentration.

The KTI on RT addresses the main issue identified in the DOE WCIS that radionuclide concentration will be reduced through depletion and dispersion. The main issue has been divided into five subissues: (i) characterizing those aspects of the physical/chemical system at YM that are likely to affect RT, (ii) identifying and evaluating processes affecting RT through fractures, (iii) identifying and evaluating processes affecting RT through porous media, (iv) identifying and evaluating processes affecting RT through alluvium, and (v) nuclear criticality issues related to transport.

The purpose of this report is to outline an approach to incorporate geochemical models in estimating sorption coefficients for RT through fractures at YM. The focus is on developing an approach that lends itself to the abstraction of processes for assessments of repository performance. Existing data on site-specific water chemistry for the saturated zone (SZ) is assumed to bound fracture water chemistry and combined with models developed for radionuclide sorption on aluminosilicates. The model results then are used to estimate sorption coefficients (K_D) appropriate to the ambient conditions in the fracture system at YM. This relatively simple approach can be used to constrain the type of probability density functions (PDFs) of sorption coefficients assumed for PA and to place reasonable upper and lower limits on the PDFs.

2 PHYSICAL/CHEMICAL CHARACTERISTICS OF THE FRACTURE SYSTEM IN THE YUCCA MOUNTAIN VICINITY

Current PA abstractions rely on empirically determined parameters (e.g.,K_D in mL/g) to describe radionuclide sorption. Experimental and modeling studies of actinide sorption indicate, however, that sorption behavior (and the parameter values that describe it) is strongly dependent on several physical and chemical properties along potential transport paths, including pH, solid-mass to solution-volume ratio (M/V), and total inorganic carbon concentration (C_T). Because abstracted PA models do not explicitly account for changes in system chemistry, the use of K_D values that may be extrapolations of laboratory data beyond experimental conditions makes the results of PA calculations uncertain. Where K_D values are not constrained by geochemistry, PA abstractions are focused on assuming conservative values (i.e., $K_D = 0$), that may not be realistic.

2.1 FRACTURE MINERALOGY

Fracture mineralogy studies at YM have focused on the Tertiary volcanic tuffs, including the Paintbrush Group, the Calico Hills Formation, and the Crater Flat Group, and are based on a suite of seven drill holes (Vaniman et al., 1996). Calcite, smectite, silica minerals, zeolites, and iron and manganese oxyhydroxides line fractures in the tuffs at YM (Carlos, 1985; 1987; 1989; Carlos et al., 1991; 1993, 1995). The most common minerals are silica polymorphs (quartz, tridymite, cristobalite, and opal), zeolites (clinoptilolite, analcime, heulandite, mordenite, stellerite), calcite, and manganese oxyhydroxide (cryptomelane, hollandite, rancieite, lithiophorite). In the Paintbrush Group above the static water level (SWL), fracture mineralogy is variable and does not necessarily correlate with the surrounding matrix mineralogy. In some cases, zeolites occur in fractures even though the tuff is devitrified and nonzeolitic (Vaniman et al., 1996). Smectite is typically widespread as a fracture-lining mineral.

In the Calico Hills Formation and the Crater Flat Group, zeolite occurrences are generally limited to zeolitized matrix, and the type of fracture-lining zeolite corresponds to the matrix zeolite (e.g., clinoptilolite in fractures is limited to clinoptilolite layers). Tridymite occurs in early fractures related to lithophysal cavities and is increasingly replaced by cristobalite or quartz with depth. Manganese oxides with nonlithophysal quartz and later mordenite are common coatings of planar cooling fractures. The zeolites, mordenite, heulandite/clinoptilolite, and stellerite are dominant in later forming fractures. Smectite and calcite occur commonly in fractures as late-forming minerals in variable amounts (Carlos et al., 1991). Whereas mordenite and euhedral heulandite are common fracture minerals in the Topopah Spring Tuff above the water table, mordenite is rare and heulandite is absent from fractures in this member below the water table taken from borehole J-13 (Carlos, 1989).

In the SZ, fractures crossing zeolitic horizons tend to be dominated by zeolites similar to the surrounding matrix (Vaniman et al., 1996). Fractures that cross devitrified horizons are more complex, dominated by iron and manganese oxyhydroxides, with subordinate amounts of zeolite, smectite, and calcite. Some oxide banding in the matrix suggests diffusion from the fracture into the matrix (Vaniman et al., 1996).

The compositions of fracture minerals have been used to infer water chemistries. For example, the zeolites in the Paintbrush Group tend to be calcic in composition, while zeolites in the Calico Hills and Crater Flat units tend to be sodic. Dating of fracture mineralogy is uncertain, but fracture-lining zeolites seem to have been formed at the time of the alteration of the tuff. For example, there is a general increase to the north in analcime at the expense of clinoptilolite/mordenite that may result from hydrothermal activity related to the Timber Mountain caldera (Bish and Aronson, 1993; Vaniman et al., 1996).

2.2 FRACTURE GEOMETRY

Fracture geometry is an important control on fracture transport of radionuclides. Fracture geometry includes fracture aperture, trace length, roughness, interconnectedness, orientation, and density. Fracture geometry is defined by the scale at which observations are made, that may range from kilometers (km) to nanometers (nm). In practice, fracture geometries are usually defined in operational terms based on the techniques employed. Techniques range from analysis of satellite imagery (10s to 100s of km), to various field mapping approaches [(km to centimeters (cm)], to microscopic observations [(millimeters (mm) to nm)]. The scale at which fracture geometry is considered for RT should be chosen to be relevant to the problem at hand. It is essential to bear in mind the operational definition employed. For example, measurements of fracture density necessarily have some operational threshold of observation; fractures below that threshold should be demonstrably unimportant to the process being evaluated using the given fracture density.

Fractures at YM have been studied for over 17 yr in support of many aspects of site characterization (Sweetkind and Williams-Stroud, 1996). Initial studies were associated with surface-based mapping; most recently, detailed fracture characterization is being carried out in the Exploratory Shaft Facility (ESF). Additional fracture data are available from boreholes at the site. Because characterization is limited to exposures such as outcrops, cleared pavements, boreholes, and the ESF, available data do not represent all lithologic units equally well and it is difficult to generalize observations or to treat the data statistically for the entire YM system. Generalization is further hampered by differences in methodology and dimensionality (one-dimensional line surveys, two-dimensional pavement maps, and full periphery ESF fracture maps) (Barton et al., 1993).

For PA calculations of fracture transport, it is necessary to translate from mechanical descriptions of fracture geometries to effective hydraulic properties (e.g., hydraulic conductivity) and parameters that allow calculation of chemical interactions (e.g., effective surface areas). Methods for making such translations are not well-established. For example, surface area is an essential parameter for sorption calculations. The effective sorptive surface area depends on bulk system generalizations of the gross area of fractures along which fluids are envisioned to flow, as well as fracture roughness and the available surface areas of sorptive minerals on the fracture walls.

2.3 LIMITS TO THE FRACTURE SYSTEM WATER CHEMISTRY

Water chemistry in the fracture system at YM is not well-defined by sampling, and is perhaps better constrained using other water chemistries as analogs to expected ranges in fracture water chemistry.

2.3.1 Perched Water Chemistry as a Constraint

Water chemistry for the perched zones are reported in Yang et al. (1996a,b). Current information includes major and minor elements, stable isotopes (δD, $\delta^{18}O$, $\delta^{13}C$), and radiogenic isotopes (^{14}C, $^{87}Sr/^{86}Sr$). These data indicate that perched water major element chemistry is distinct from pore water chemistry in the unsaturated zone (UZ) (Yang et al., 1996a) and more similar to the water chemistry from the SZ (e.g., Perfect et al., 1995). In general the perched water is more dilute than the UZ pore waters, with lower chloride concentrations (about 4 to 8 mg/L, with one sample up to 15 mg/L). The lower chloride concentration suggests that the perched water forms with less interaction with the host rock, suggesting a shorter residence time that is consistent with a fracture source. The differences in water chemistry also indicate that the perched

water is not in chemical equilibrium with the pore water. Detectable bomb pulse tritium indicates that there is at least some rapid recharge of the perched water zones, and uncorrected radiogenic ^{14}C indicates a residence time of about 7,000 yr that is young relative to regional groundwaters (Yang et al., 1996a). Deuterium and ^{18}O stable isotope chemistry indicates that perched water is isotopically heavier than SZ water and close to the current YM local meteoric water line. The heavier ^{18}O values suggest that the perched water does not contain a significant portion of isotopically light water from the last ice age (10,000 yr) supporting an age of <10,000 yr, although this does not exclude the possibility of older water with an isotopic signature similar to modern values. The similarity to the modern YM local meteoric water line suggests that recharge of the perched water bodies is through local precipitation, principally during winter storm events, rather than from higher elevations to the north.

2.3.2 Saturated Zone Water Chemistry as a Constraint

A comprehensive source of SZ water chemistry data is found in the United States Geological Survey (USGS) report of Perfect et al. (1995). This report includes compressed spreadsheet files formatted using the Lotus 1-2-3 commercial software package (Lotus Corporation). Data contained in the spreadsheet file are major and minor element analyses compiled over several decades for the region surrounding YM. One input file contains the raw data for over 4,700 wells and springs from USGS and Department of Energy (DOE) reports and the USGS National Water Information Service (NWIS) database (Perfect et al., 1995). The data file has been edited by Perfect et al. (1995) to remove duplicates, make chemical data entries consistent, and calculate charge balance. The editing philosophy used by Perfect et al. (1995) is described in their report. The Perfect et al. (1995) data were not generally collected under a DOE-approved quality assurance (QA) program, but are freely used here. The sources referenced in Perfect et al. (1995) should be consulted for determining the quality of the data.

The water samples as recorded in Perfect et al. (1995) are typically integrated samples. Depth to water is sometimes indicated, but the depth to the producing horizon is not generally given. Only a few samples were collected from distinct intervals isolated by packers. For this reason, it is likely that the water chemistries reported are for a mixture of fracture and pore water. Without more detailed information on producing horizons and the presence of fractured production zones, it is impossible to define any regional-scale differences that may exist between fracture and pore water chemistry. For the purposes of this report, given the similarity between perched water that are likely to be recharged through fractures and SZ water chemistry, the chemical ranges represented in the Perfect et al. (1995) database are assumed to represent the total variation that is likely in waters in the YM fracture system. This assumption is also supported by the observation of Murphy and Pabalan (1994) of chemical similarities between fracture water collected at Rainier Mesa (White et al., 1980) and SZ groundwater at YM.

A first step in using the database of Perfect et al. (1995) to investigate sorption was to screen and cull the data to develop a more refined database of complete water analyses suitable for geochemical modeling. The entire edited database (DATAEDIT.WK1) of Perfect et al. (1995) includes 3,733 groundwater analyses. For ease of manipulation, these analyses were sorted on north-south location and assigned a unique identification number from 1 (southernmost) to 3,733 (northernmost). Many of the analyses are replicate samples collected at different times from springs and wells. Complete major and minor element concentrations are commonly reported but, in some instances, only trace contaminants such as Cd, Cu, and Zn were reported for a given analyses. All concentrations are reported in mg/L, and -99998 indicates no reported value. Based on criteria presented in Hitchon and Brulotte (1994), we used a series of steps

table 2-1) to eliminate unsuitable water analyses from the database. The number of analyses eliminated by each screening criteria is also listed in table 2-1.

It is important to note that these criteria are not necessarily mutually exclusive and that, although the total number of analyses eliminated will remain the same, the number of analyses eliminated for a given criterion is dependent on the order in which the steps were taken. For example, Perfect et al. (1995) report that 1,373 records did not charge balance to within 10 percent. These include analyses without reported pH values as well as analyses missing major elements such as Ca, Mg, Na, and Cl. If charge balance had been the first criterion used, the number of analyses eliminated by the other criteria would have been significantly fewer.

As developed by Perfect et al. (1995), sample locations are indicated with latitude and longitude given in degrees, minutes, and seconds. A spreadsheet macro was developed in Excel, Version 5.0 (Microsoft Corporation) to convert these locations first to decimal degrees [degrees + (minutes/60) + (seconds/3,600)], and then project the locations to Universal Transverse Mercator (UTM) coordinates. The UTM projection conversion is based on UTM Zone 11, with a 500,000 meters false easting, a central meridian of -117° W, and using the Clarke 1866 ellipsoid. The formulas used in the conversion were taken from, and checked against, examples given in Snyder (1987). The conversion is accurate, but the accuracy with which a given sample is located is limited by the original degree-minute-second location in Perfect et al. (1995). For examples, a second of latitude represents a distance of about 30 m. The area covered by the dataset culled using geochemical screening criteria (n = 956 analyses) covers a large area extending from 3,879,865N to 4,202,513N and 436,141E to 679,985E, a total of almost 79,000 km^2. With the UTM coordinates, an additional culling criteria that can be used is to limit the study to those waters within the YM vicinity. A 100 km × 100 km area is considered, with UTM coordinates from 4,000,000N to 4,100,000N and 500,000E to 600,000E. This eliminates an additional 496 analyses for a remaining total of 460. These include multiple analyses for the same well/spring, and no attempt has yet been made to select a preferred analysis or calculate a mean water composition for a given sampling point.

2.4 REGIONAL GROUNDWATER—MEASURED GEOCHEMICAL PARAMETERS

PA calculations typically rely on PDFs to describe the physical system at YM. A similar approach to geochemical parameters ultimately may be used to incorporate indirectly more detailed geochemical models in PA (see discussion in section 4). The database of water chemistries at YM can be used to identify current ranges and distribution types for key measured geochemical parameters, including pH and component concentrations. A brief description of several key geochemical parameters is provided here. Descriptive statistics calculated by Excel, Version 5.0 are included in table 2-2. In this report, distributions are described in qualitative terms using best-fit-to-eye. Similar values for mean, median, and mode support a normal (or log-normal) distribution. Non-zero vales for skewness suggest a non-normal distribution. It is important to remember that water samples are typically integrated over a large interval in the well, and local horizons of higher or lower component concentration may not be distinguishable. This approach also does not address spatial heterogeneity of the water chemistry. Spatial analysis with a geographic information system such as ArcInfo (Environmental Systems Research Institute, Inc.) may reveal trends in geochemical parameters that are likely to control RT.

Table 2-1. Screening and culling criteria used with DATAEDIT.WK1 hydrochemistry database of Perfect et al. (1995), as modified from Hitchon and Brulotte (1994)

Elimination Criteria	Number of Analyses Eliminated	Remaining Analyses (from 3,733)
No pH; pH <5 or pH >10	1,708	2,025
No reported Ca	121	1,904
No reported Mg	127	1,777
No reported Cl	9	1,768
No reported SO_4	21	1,747
No reported Na	44	1,703
No reported HCO_3 or CO_3	405	1,298
Not charge balanced (± 10 %)	23	1,275
No collection date reported	82	1,193
Collected before 1960	165	1,027
Mg > Ca	72	956
UTM Coordinates: 4,000,000N to 4,100,000N 500,000E to 600,000E	496	460

2.4.1 pH

Measured pH is a key parameter that controls chemical processes such as sorption and mineral precipitation that affect RT (e.g., Turner, 1995 and references therein). For the culled database described earlier in table 2-1 (n = 460 samples), the minimum and maximum pH are 6.3 to 9.6 (see the first culling criterion in table 2-1). A histogram shows a best-fit-to-eye normal distribution for pH (figure 2-1), which is equivalent to a log-normal distribution for H^+ activity. Perfect et al. (1995) noted that they have not attempted to distinguish between laboratory and field pH measurements; problems due to degassing of CO_2 may exist but not be readily discernible in the dataset.

2.4.2 Total Inorganic Carbon

Groundwater C_T is linked to pH through aqueous carbonate chemistry, and can also affect retardation processes such as sorption and mineral precipitation. Groundwater C_T in the system exhibits roughly a best-fit-to-eye lognormal distribution (figure 2-2) over a very broad range of 6.8 to more than 10,000 mg/L. However, the total number of analyses with C_T > 1,000 mg/L is small (10 out of 460 samples) and gives a large positive skewness to the distribution (table 2-2). Given that these high-concentration samples are likely

Table 2-2. Descriptive statistics of measured groundwater chemical parameters

	pH (standard units)	C_T (mg/L)	SiO_2 (mg/L)
Mean	7.83	295.76	43.21
Standard Error	0.02	24.52	0.99
Median	7.8	245.0	43.0
Mode	7.8	300.0	22.0
Standard Deviation	0.45	525.99	21.25
Kurtosis	1.75	270.67	-1.30
Skewness	0.43	15.03	0.14
Range	3.3	10133.20	78.30
Minimum	6.3	6.80	3.70
Maximum	9.6	10140.00	82.0
Count	460	460	457

to be brines collected from playa deposits (29,000 mg/L > Na concentration > 1,000 mg/L), they are likely not to be representative of deep regional groundwaters or fracture waters, and are certainly unusable as a potable water source.

2.4.3 Aqueous Silica

Aqueous silica may have an effect on the mineral phases that may control radionuclide solubility (e.g., uranophane), and may also limit the occurrence of sorbing minerals such as zeolites and clays. Silica may also precipitate and plug fracture porosity. The culling criteria described earlier did not screen for analyses with no reported aqueous SiO_2 concentrations, but almost all of the analyses (457 of 460) provided a measurement. SiO_2 concentration ranges from 2 to 130 mg/L. The distribution is bimodal in appearance, with one peak at about 20–30 mg/L and a second at about 60–70 mg/L (figure 2-3). Multimodal distributions such as this perhaps are best handled in PA analyses through the use of a look-up table.

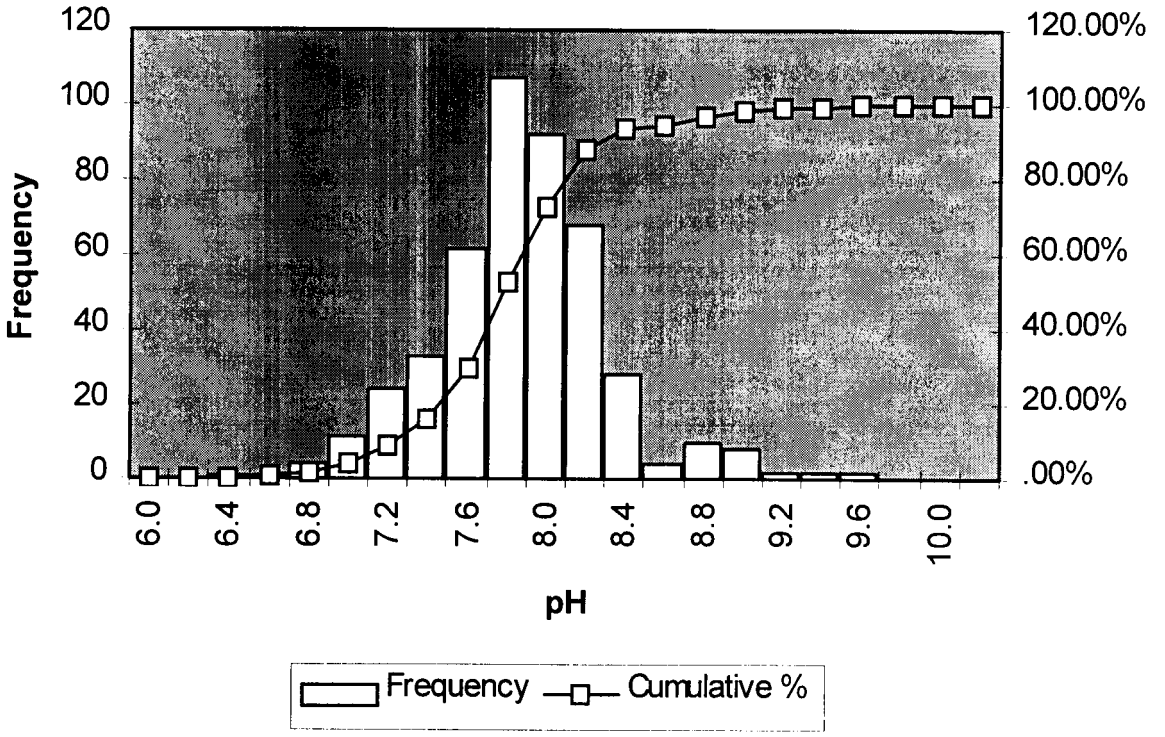

Figure 2-1. Distribution of pH for saturated zone regional groundwaters (data from Perfect et al., 1995; see text for details).

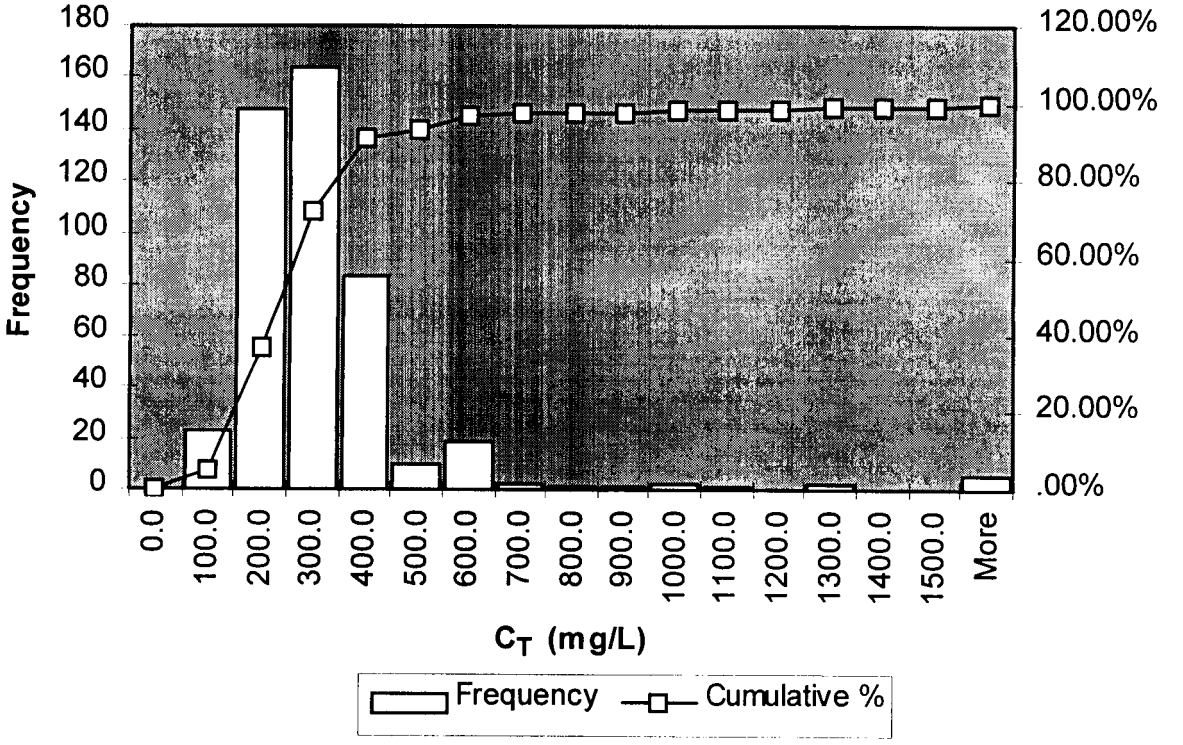

Figure 2-2. Distribution of total inorganic carbon (C_T in mg/L) for saturated zone regional groundwaters (data from Perfect et al., 1995; see text for details).

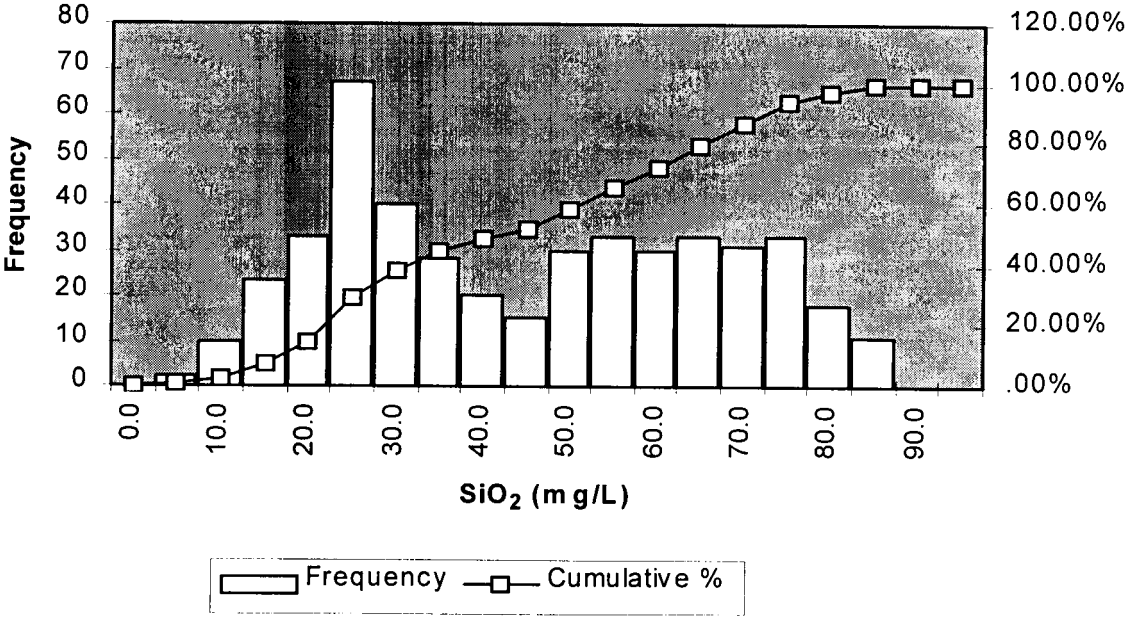

Figure 2-3. Distribution of SiO_2 (in mg/L) for saturated zone regional groundwaters (data from Perfect et al., 1995; see text for details).

3 REGIONAL GROUNDWATER—DERIVED GEOCHEMICAL PARAMETERS

To examine the degree of chemical speciation and saturation with respect to minerals that may be critical for the purposes of RT through the fracture system, the major elements Ca, Mg, Na, K, HCO_3^-, CO_3^{2-}, SO_4^{2-}, Cl, F, Fe, and SiO_2(aq) were written to an input file appropriately formatted for MINTEQA2, Version 3.11 (Allison et al., 1991). For each analysis, the pH and temperature were fixed at the measured values; Eh was unspecified due to a lack of measured data, and measured Fe was assumed to be entirely Fe^{3+}. Output from MINTEQA2 includes equilibrium ionic strength, gas partial pressures, and saturation indices for minerals in the MINTEQA2 database. The output files for 460 separate analyses are too large to be convenient, and derived geochemical parameters were extracted for ease of handling. Descriptive statistics of the derived geochemical parameters calculated by Excel, Version 5.0, are included in table 3-1.

3.1 IONIC STRENGTH

Ionic strength has relatively little effect on actinide surface complexation (Pabalan et al., 1998), but changes in ionic strength can affect other transport processes that influence RT such as sorption by ion exchange and colloid stability. Part of the MINTEQA2 output is the equilibrium ionic strength which takes into account the predicted speciation. Based on the major and minor elements provided in the analyses of Perfect et al. (1995), calculated equilibrium ionic strength ranges from to 4.34×10^{-4} molal in the most dilute groundwaters to about 1.3 molal for brines collected in playa deposits (table 3-1). The upper limit should be considered only as approximate since the Davies equation activity coefficient used by MINTEQA2 is not strictly applicable at ionic strength greater than about 0.5 molal (Allison et al., 1991). Most of the groundwaters are dilute, however, with only 3 out of 460 samples exceeding 0.5 molal, and the few brines are unpotable and unlikely to play a significant role in the transport path. The distribution of the ionic strength is best-fit-to-eye log-normal, with a mean value of about 8×10^{-3} molal (figure 3-1).

3.2 LOG PCO_2

The partial pressure of CO_2 (PCO_2) is a measure of the amount of inorganic carbon in the aqueous system, and is related to pH and C_T through aqueous carbonate geochemistry. Although there are some values at or below atmospheric levels [PCO_2(atmospheric) = $10^{-3.5}$ atm], the bulk of the groundwaters in the YM vicinity exhibit much higher PCO_2. As noted by Murphy and Pabalan (1994), excess CO_2 in tuffaceous aquifers likely is derived during recharge, primarily from soil-zone biological processes such as root respiration. High carbonate (and PCO_2) levels may also result from wells that tap Paleozoic carbonate aquifers. For example, UE-25 p#1 penetrates the Silurian dolomites to the east of YM, and has an above-average calculated PCO_2 of $10^{-1.78}$ atm. The distribution is best-fit-to-eye log-normal, with a mean value of $10^{-2.5}$ atm, an order of magnitude greater than atmospheric values (figure 3-2).

3.3 SATURATION INDICES

The presence or absence of several different minerals may influence retardation in fractures at YM. One measure of the stability of a mineral in a water of a given chemistry is the saturation index (SI), represented by:

Table 3-1. Descriptive statistics of calculated groundwater chemical parameters

	Log (Equilibrium Ionic Strength) (molal)	Log PCO_2 (atm)
Mean	-2.09	-2.50
Standard Error	0.02	0.03
Median	-2.07	-2.45
Mode	-1.99	-2.34
Standard Deviation	0.39	0.54
Kurtosis	8.07	3.73
Skewness	1.09	-1.30
Range	3.48	4.311
Minimum	-3.36	-5.08
Maximum	0.12	-0.77
Count	460	460

$$\mathbf{SI} = \mathbf{log}\left(\frac{\mathbf{IAP}}{\mathbf{K_{eq}}}\right) \tag{3-1}$$

where IAP is the ion activity product and K_{eq} is the equilibrium constant for the dissolution/precipitation reaction. When SI > 0, the groundwater is chemically saturated with respect to a given phase; SI < 0 indicates undersaturation, and SI = 0 indicates the system is at chemical equilibrium with respect to the mineral of interest.

3.3.1 Calcite

Calculated SI values with respect to calcite, for the regional groundwaters, are shown in figure 3-3. Calcite is potentially a strong sorber for neptunium (Triay et al. 1996a), and it occurs as a fracture-filling mineral in the YM fracture system (Vaniman et al., 1996). Calcite dissolves readily and does not require large supersaturations to precipitate. For a smaller dataset than that considered in this report, Murphy (1995) noted that waters collected from wells in the tuffaceous aquifers immediately around the proposed repository are undersaturated with respect to calcite, and used the occurrence of calcite as evidence of channelized flow

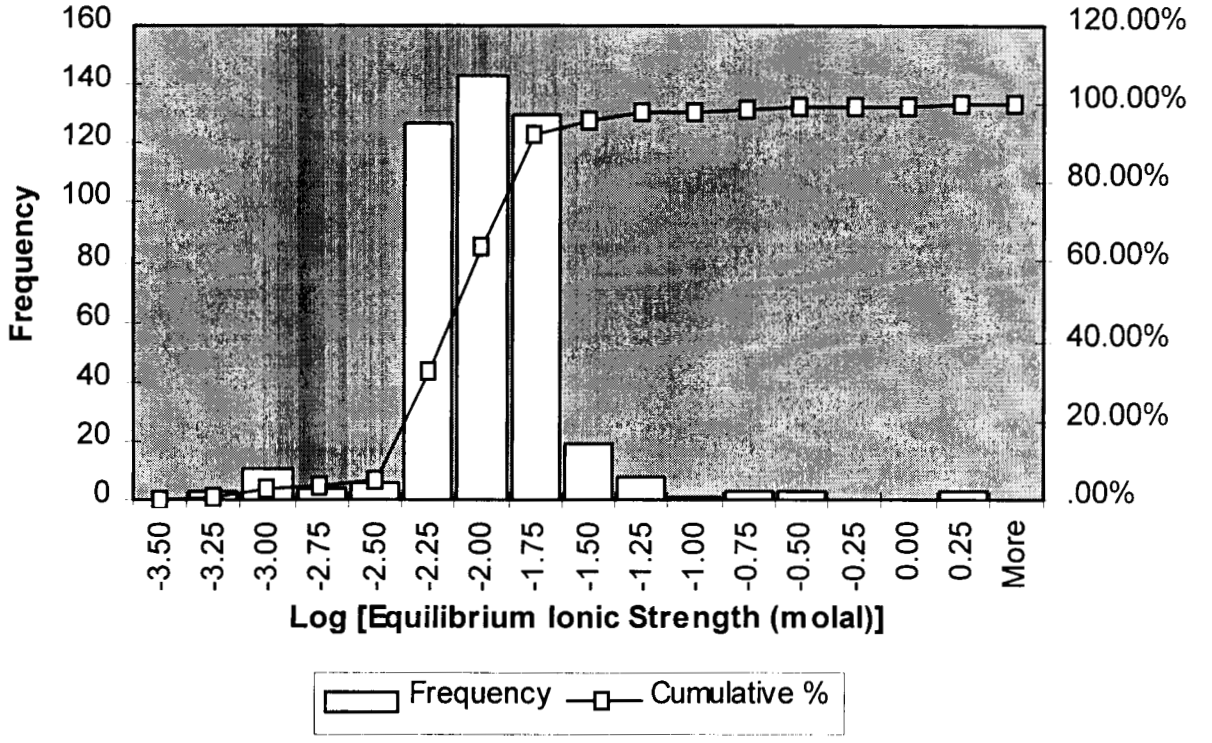

Figure 3-1. Distribution of the logarithm of the equilibrium ionic strength for saturated zone regional groundwaters (data from Perfect et al., 1995; see text for details) calculated using MINTEQA2 (Allison et al., 1991).

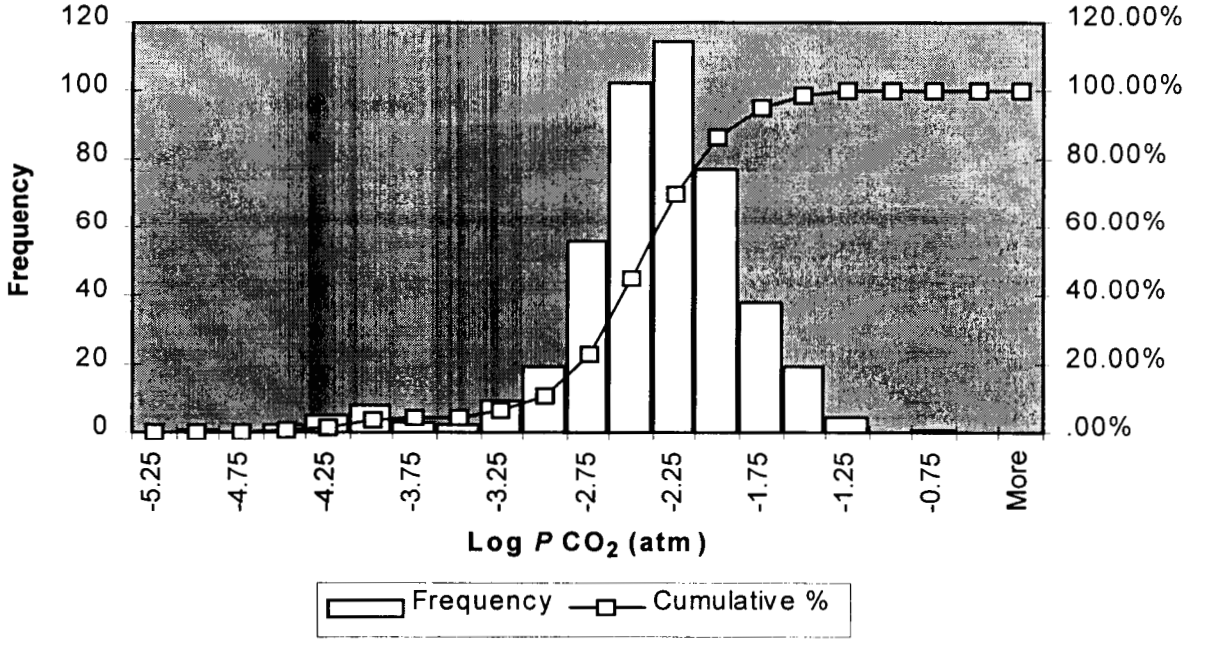

Figure 3-2. Distribution of Log PCO_2(in atmospheres) for saturated zone regional groundwaters (data from Perfect et al., 1995; see text for details) calculated using MINTEQA2 (Allison et al., 1991).

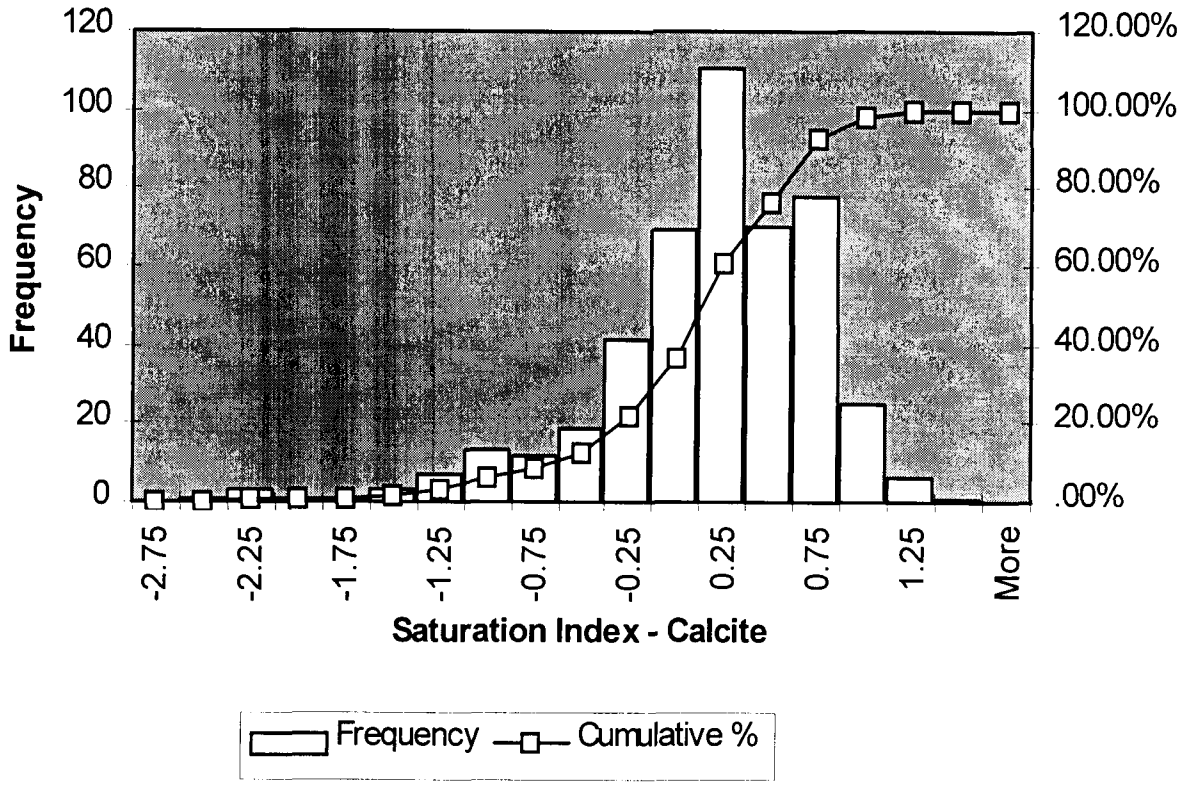

Figure 3-3. Distribution of the Saturation Index for calcite for saturated zone regional groundwaters (data from Perfect et al., 1995; see text for details) calculated using MINTEQA2 (Allison et al., 1991).

in the groundwater. As shown in figure 3-3, however, most of the groundwater samples (about 360 out of 460) in the YM vicinity are saturated and supersaturated with respect to calcite (SI > 0). The distribution is best-fit-to-eye normal, with a mean SI of about 0.06. The standard deviation is 0.6, suggesting that a majority of the waters are near equlibrium with calcite.

It is important to note that the waters reported in Perfect et al. (1995) may include waters from springs and wells that tap into Paleozoic carbonate aquifers that are expected to be saturated with respect to calcite whereas the waters used by Murphy (1995) are limited to those from tuffaceous aquifers.

3.3.2 Fe-Oxides

Iron oxyhydroxides are an important potential sorptive mineral in the YM fracture system. All water analyses that report Fe concentrations are calculated to be supersaturated with respect to iron oxyhydroxides such as hematite, goethite, and lepidocrocite, consistent with their common occurrence as fracture lining minerals (Vaniman et al., 1996). The calculated SI values should be considered as maximums due to the assumption that all reported Fe is in the form of Fe^{3+}. Analyses of Fe^{2+}, Fe^{3+}, and/or measured Eh are not reported in Perfect et al. (1995), and would be necessary to more realistically constrain SI for Fe-oxyhydroxides.

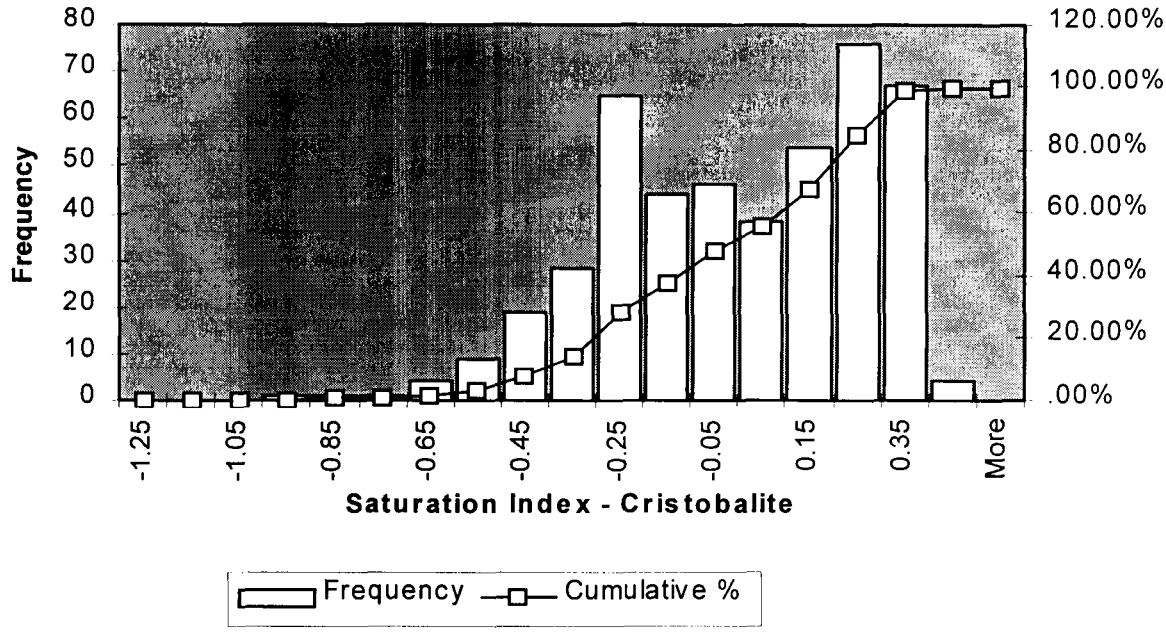

Figure 3-4. Distribution of the Saturation Index for cristobalite for saturated zone regional groundwaters (data from Perfect et al., 1995; see text for details) calculated using MINTEQA2 (Allison et al., 1991).

3.3.3 Cristobalite

Cristobalite is both a common rock-forming mineral in the YM tuffs and a fracture-filling mineral (Vaniman et al., 1996). Dissolution of cristobalite and redistribution of silica may also have an effect on fracture mineralogy. The calculated SI for cristobalite is shown in figure 3-4. The distribution is bimodal, with one peak at a slightly undersaturated SI of -0.25. The second peak in the distribution is at a slightly supersaturated level with a SI of 0.25. It is not clear from the data presented in figure 3-4, but this bimodal distribution may reflect different water sources, with cristobalite-saturated groundwaters collected from tuffaceous aquifers or alluvial aquifers made up predominantly of tuffs. Cristobalite-undersaturated groundwaters are likely to be collected from Paleozoic carbonate aquifers or from alluvial aquifers made up of carbonate host rock. Spatial analysis of the surface geology at different sample locations may provide a measure of water type, but identification of sampled aquifers in wells is necessary to fully evaluate water sources. Again, a look-up table may be the best means of assessing this type of multimodal distribution in PA abstractions.

3.3.4 Gypsum

Gypsum may have an effect on RT by precipitating in fractures and plugging available porosity. All the groundwaters collected in the YM vicinity are undersaturated with respect to gypsum. This is consistent with the lack of subsurface evaporite deposits and with the reported absence of gypsum in tuffaceous aquifers (Vaniman et al., 1996).

3.4 COLLOIDAL PARTICLE CONCENTRATIONS

Colloid transport of radionuclides through fractured tuff has been suggested by field tests conducted to the north of YM at Pahute Mesa on the Nevada Test Site. Ultrafiltration of groundwaters pumped from wells downgradient from an underground detonation cavity indicate that isotopes of Co, Cs, Eu, and Pu were detected on natural colloidal material consisting of mordenite, illite, and cristobalite (Buddemeier and Hunt, 1988; Kersting and Thompson, 1997; Smith, 1997). Tracer tests at the C-well complex (UE-25 c#1, c#2, and c#3) have also demonstrated that colloid-sized particles (0.36-μm-diameter polystyrene microspheres) migrated 31.7 m through the Lower Bullfrog Tuff, but were attenuated by filtration, with only about 11 percent recovery after 2,650 hr (Reimus and Turin, 1997).

If actinides and other radioelements can sorb onto natural colloids, the stability of the particles in suspension is of critical importance in colloid-mediated transport. The stability of the colloidal suspension of charged particles varies as a function of ionic strength, groundwater chemistry, and pH. For example, at low ionic strengths, the electrostatic double-layer (EDL) expands outward from particle surfaces, stabilizing the colloids in suspension through electrostatic repulsion. At higher ionic strengths, the double layer collapses, and the charged particles begin to flocculate (agglomerate) and come out of suspension due to gravity settling and filtration. Variations in overall solution chemistry (pH, component concentrations) and moisture content of the medium influence the magnitude of the ionic strength effect.

Assuming that ionic strength is the principal control on colloid stability, Triay (1998) presented a relationship between colloid particle concentration (particles/mL) and ionic strength (molal), expressed as:

$$\textbf{log[coll] (particles/mL)} = \textbf{7.0} - \textbf{34} \times \textit{I.S.}\ \textbf{(molal)} \qquad (3\text{-}2)$$

This empirical relationship is based on observed colloid particle concentrations and groundwater ionic strength for field sites in a variety of rock/water systems throughout the world. Applying the relationship in Eq. (3-2) with the calculated equilibrium ionic strength for groundwaters in the YM vicinity (section 3.1) results in the predicted particle concentration distribution shown in figure 3-5. For example, the mean predicted particle concentration is about $10^{6.3}$ particles/mL and the median value is about $10^{6.7}$ particles/mL, comparable to the particle concentration of $10^{6.6}$ particles/mL reported for the 100- to 500-nm size fraction in J-13 well water (Triay et al., 1996b). The total predicted range in colloid concentrations is very large, and the distribution is negatively skewed by the values at the lower end of the range. For example, the maximum estimated particle concentration is about $10^{7.0}$ particles/mL, slightly greater that the mean/median, but many orders of magnitude greater than the estimated minimum ($<10^{-30}$ particles/mL). This narrow range for the bulk of the samples is a direct consequence of the relatively restricted range in equilibrium ionic strength (figure 3-1). The relatively few higher ionic strength groundwaters (<10 analyses) account for the very small colloid concentrations shown in figure 3-5.

It is important to remember that the predicted distribution shown in figure 3-5 is based on a simplified empirical relationship between groundwater chemistry and colloid particle concentrations, and is restricted to only one chemical parameter, ionic strength. Other parameters that may have an effect on log[coll], such as pH and relative concentrations of alkali (Na^+) and alkaline earth (Ca^{2+}) elements (Degueldre et al., 1996; Degueldre, 1997), are not included in this analysis. Additional investigation to characterize the relationship between colloid stability and other chemical parameters is necessary to make a more quantitative estimate of log[coll]. Finally, the estimate of particle concentration is only part of the information needed to evaluate

radionuclide colloid transport. Particle size distribution and surface area estimates are necessary to calculate the amount of radionuclides that can be loaded onto the colloid particles and the efficiency with which they are transported through the YM fracture system. The information shown in figure 3-5 should be considered as a qualitative estimate of the range and distribution type that may be observed for particle concentrations, and therefore colloid stability, in the groundwaters near YM.

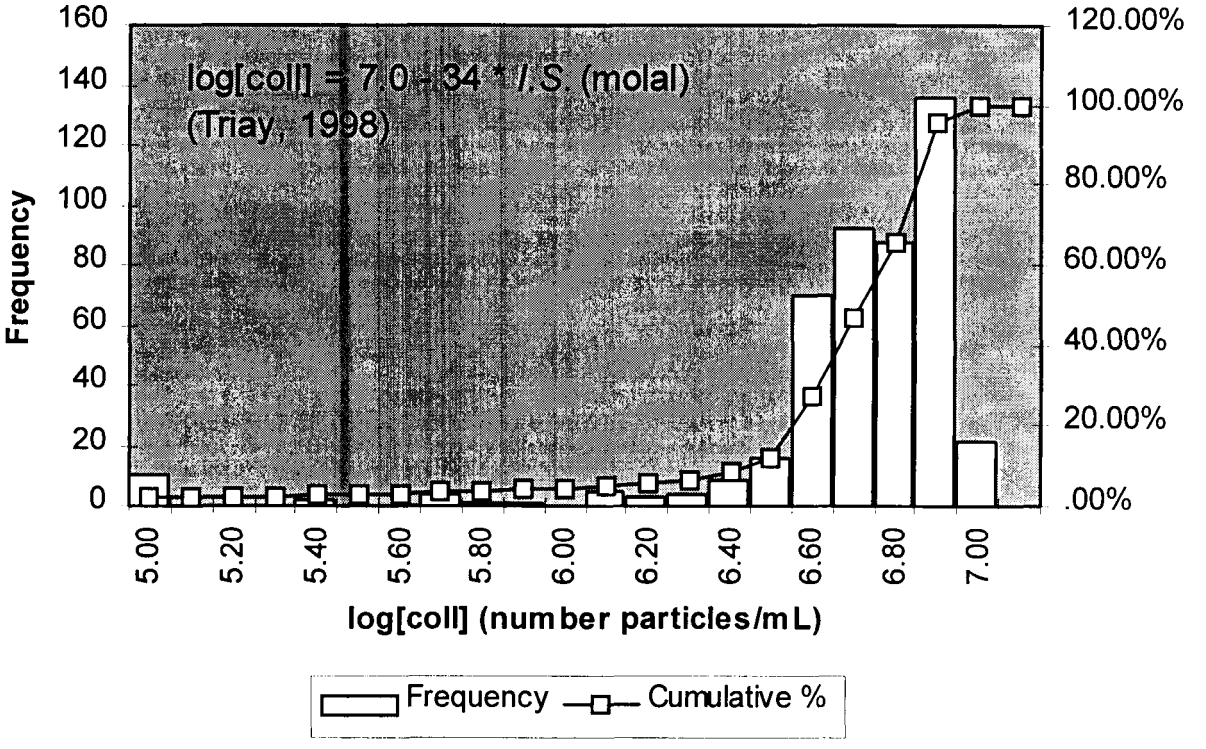

Figure 3-5. Colloid particle concentration (particles/mL) based on the empirical relationship between colloid particles and ionic strength (molal) presented by Triay (1998). Ionic strength is based on the equilibrium ionic strength (see figure 3-1) calculated for water chemistries from Perfect et al. (1995). See section 3.1 for details.

4 FRACTURE RETARDATION—MODELING APPROACHES

Ideally, mechanistic sorption models would be directly incorporated into reactive transport codes. While hydrogeochemical transport codes may be used to examine particular aspects of reactive transport, the additional computational burden that results from coupling equations for geochemistry and fluid flow may be excessive for the purposes of PA. This is even more important for stochastic approaches that rely on sampling techniques and many realizations to generate Complementary Cumulative Distribution Functions (CCDFs) and population statistics. It may be possible to use a geochemical sorption model "off-line" to support K_D selection and to assess the effect of critical parameters such as pH and C_T for site-specific conditions. There are two methods for this type of indirect incorporation of geochemical sorption models into PA: (i) it may be possible to use a sorption model to extrapolate over a wide range in geochemical conditions, creating a "response surface" as a function of key geochemical parameters that can be sampled in PA; (ii) given existing site-specific information on the physical/chemical system at YM, sorption models can be used to calculate sorption parameters and to provide realistic constraints on the type and statistical parameters defining the PDFs used to describe sorption in PA. The first approach is perhaps more appropriate for predictive modeling, but will require modification of existing PA codes. The second approach can be used to modify existing PDFs and more quickly can be incorporated into current PA codes. The second approach is a step towards incorporating geochemical constraints in PA, and is the focus of this report. The first approach will be discussed in a subsequent report.

4.1 KEY GEOCHEMICAL PARAMETERS

The distribution (or sorption) coefficient (K_D) is a convenient empirical ratio for representation of sorption data and is commonly used to represent retardation in transport models used in PA. The K_D (mL/g) can be defined as:

$$K_D(\text{mL/g}) = \frac{\text{equilibrium mass of radionuclide sorbed on solid}}{\text{equilibrium mass of radionuclide in solution}} \times \left(\frac{V}{M}\right) \qquad (4\text{-}1)$$

where V is the volume of experimental solution in mL, and M is the mass of solid in g. The use of K_D has the effect of normalizing sorption results to the M/V used in laboratory batch experiments and provides a means of accounting for the change in solution concentration that occurs during the course of the experiment. Results are presented in the following sections in terms of K_D versus pH or in terms of $K_{A'}$ (mL/m^2) versus pH, where $K_{A'}$ is K_D normalized to the mineral's "effective" measured specific surface area (A') (i.e., $K_{A'} = K_D/A'$) (Bertetti et al., 1998; Pabalan et al., 1998).

In PA studies, contaminant sorption is typically modeled assuming a constant K_D for a given radionuclide for each hydrostratigraphic unit (e.g., Wilson et al., 1994; TRW Environmental Safety Systems, Inc., 1995; Wescott et al., 1995). This approach readily is incorporated into existing transport codes and simplifies the numerical simulation of radionuclide migration. It is well-recognized, however, that sorption is dependent on the specific geochemical conditions of the transport path instead of being constant for a given rock type. For example, experimental results show a link between the aqueous speciation of an actinide and its sorption behavior (Pabalan et al., 1998; Bertetti et al., 1998). Actinide sorption is important under conditions in which actinyl-hydroxy complexes are favored to form in the aqueous phase. Geochemical conditions which inhibit the formation of actinyl-hydroxy complexes, e.g., low pH and carbonate complex

formation, suppress actinide sorption. The similarity in the pH-dependence of actinide sorption on a wide variety of minerals such as quartz, α-alumina, clinoptilolite, montmorillonite, amorphous silica, kaolinite, and titanium oxide, which are substrates of distinct surface charge properties, suggests that actinide sorption is not sensitive to the surface charge characteristics of the sorbent as compared to the effect of changing the total number of available sites. When expressed in terms of K_D or $K_{A'}$, experimental and modeling results demonstrate that changing M/V has little influence on actinide sorption, except at very low values (Bertetti et al., 1998; Pabalan et al., 1998). Ionic strength effects are limited for actinide surface complexation reactions, although these effects can be important if ion-exchange is the predominant sorption mechanism. The data derived from the literature suggest that the magnitudes of actinide sorption (at a specific pH, initial radionuclide concentration, and PCO_2) are the same for different minerals if normalized to the "effective" surface area (A′), deriving the parameter K_A' (mL/m^2) (Bertetti et al., 1998; Pabalan et al., 1998).

4.2 SURFACE COMPLEXATION MODELING APPROACHES

The strong pH-dependence observed in sorption experiments indicates that predictive sorption modeling requires geochemical models capable of simulating the influence of changing physicochemical conditions on actinide aqueous speciation and sorption. Although actinide sorption appears relatively insensitive to surface charge, a class of models that has been used with success in modeling pH-dependent sorption is the electrostatic surface complexation model (SCM) (Davis and Leckie, 1978; Westall and Hohl, 1980; Davis and Kent, 1990; Hayes et al., 1991; Turner, 1995).

4.2.1 Model Description

SCMs are based on the assumption of analogous behavior between aqueous complex formation in the bulk solution and formation of surface complexes with functional binding sites at the mineral-water interface. Surface reactions are written for sorbing species, and mass action and mass balance relations are used to determine sorption at the mineral surface as a function of system chemistry. Of the different SCMs, the Diffuse-Layer Model (DLM) is perhaps the simplest, using a two-layer representation of the mineral-water interface. The pH-dependence of surface charge development is accounted for in the DLM but, in contrast to more complex multi-layer models, the DLM assumes that supporting electrolytes such as Na^+ and Cl^- do not interact with the surface. For this reason, the DLM neglects the possible formation of outer-sphere complexes involving the background electrolytes and does not specifically address the effects of ionic strength on sorption except through the charge-potential relationship (Davis and Kent, 1990; Dzombak and Morel, 1990). The details of the DLM and the simplified approach used in this study are described elsewhere (Davis and Kent, 1990; Dzombak and Morel, 1990; Turner and Sassman, 1996) and only a brief overview of the DLM as applied to neptunium sorption is presented here.

A generalized pH-dependent sorption reaction between aqueous actinides and a variably charged surface sorption site can be represented by Np(V) and written in the form:

$$>XOH^\circ + pNpO_2^+ + nH_2O \leftrightharpoons [>XOH_q\text{-}(NpO_2)_p(OH)_n]^{p+q-n-1} + (1+n-q)H^+ \qquad (4\text{-}2)$$

where q is the protonation state of the sorption site (q = 0, 1, or 2 for deprotonated, neutral, and protonated sites, respectively), and p and n are the reaction coefficients for NpO_2^+ and H_2O, respectively. NpO_2^+ and

$[>XOH_q\text{-}(NpO_2)_p(OH)_n]^{p+q-n-1}$ represent the aqueous Np(V) species and the Np(V) surface complex, respectively. In the SCM approach, a coulombic correction is incorporated into the mass action expressions for surface reactions to extract the intrinsic equilibrium constants (e.g., K_+^{int}, K_-^{int} and $K^{int}_{[>XOH_q\text{-}(NpO_2)_p(OH)_n]}$ that are independent of surface charge. For sorption reactions of the type given in Eq. (4-2), $K^{int}_{[>XOH_q\text{-}(NpO_2)_p(OH)_n]}$ is commonly referred to as the binding constant. Similar reactions can be written for other actinides such as uranium and plutonium.

The DLM has been used to simulate Np(V) and U(VI) sorption on montmorillonite (Turner et al., 1998; Pabalan and Turner, 1997). Montmorillonite is a common fracture mineral in volcanic tuffs in the YM vicinity (Bish et al., 1996; Vaniman et al., 1996), and is probably also present in the alluvium derived from volcanic outcrop. The observed dependence of Np(V)- and U(VI)-montmorillonite sorption on pH and PCO_2 is a consequence of mass action effects and equilibrium chemistry in the actinide-H_2O-CO_2-montmorillonite system represented by Eq. (4-2). In a qualitative sense, an increase in the activity of NpO_2^+ (or similarly UO_2^{2+}) drives the equilibrium reaction in Eq. (4-2) forward (increasing sorption). The presence of a complexing ligand such as dissolved carbonate in the presence of a CO_2 atmosphere tends to form aqueous actinide-carbonate complexes in competition with the sorbing clay surface. Carbonate competition for the available actinide increases with increasing pH, reducing the aqueous activity of NpO_2^+ or UO_2^{2+} and driving the reaction in the opposite direction (decreasing sorption). This explanation of course, is simplistic due to the synergistic effects between solution chemistry, sorption site protonation state, and speciation of the aqueous and surface complexes.

4.2.2 Sorption Modeling—Diffuse-Layer Model Parameters

Modeling for the regional groundwaters in the YM vicinity was performed for both Np(V) and U(VI) sorption on montmorillonite using the DLM as discussed above. MINTEQA2, Version 3.11 (Allison et al., 1991) was used in the same manner as that described in section 3, with major element water chemistry from the culled data set of Perfect et al. (1995) formatted for MINTEQA2 input (460 analyses). Surface sorption reactions, based on Center for Nuclear Waste Regulatory Analyses (CNWRA) experimental work (Pabalan and Turner, 1997; Turner et al., 1998), were added to the input file. Total dissolved and sorbed concentrations were extracted from the output file for ease of handling.

Parameters and reference sources for the model are given in table 4-1. For the purposes of modeling, a dilute concentration of 10^{-6} molal was assumed for Np(V) and U(VI) concentrations. This is likely to be low enough to avoid the complications of precipitation and is consistent with solubility ranges assumed for Total Performance Assessment (TPA). There is also experimental and modeling evidence to suggest that surface complexation is relatively insensitive to actinide concentrations $<10^{-5}$ molal (Turner, 1995; Pabalan and Turner, 1997). It is important to note that, although full aqueous speciation is included in the model, the only surface reactions considered in the model are protonation/deprotonation and radionuclide sorption reactions. No competitive sorption reactions are incorporated in the model due to a general lack of available information on sorption behavior for the H_2O–CO_2-montmorillonite system. Therefore, predicted changes in sorption behavior are limited to those resulting from aqueous complexation of the radionuclide with ligands in the groundwater (Pabalan and Turner, 1997; Turner et al., 1998). DLM results are also dependent upon the thermodynamic data that are used in constructing the model. The thermodynamic data for Np(V) and U(VI) are taken from the MINTEQA2 database modified at the CNWRA (Turner, 1993), with exceptions as noted in Pabalan and Turner (1997) and Turner et al. (1998).

Table 4-1. Diffuse-Layer Model parameters used in modeling Np(V) and U(VI) sorption on montmorillonite

Model Parameter/Surface Reaction	Mineral/Surface Parameters	
Solid concentration (M/V)	1 g/L	
Site density	2.3 sites/nm^2	
Surface area[a]	9.7 m^2/g	
Total site concentration	>AlOH^o = 1.69 × 10^{-5} mol sites/L >SiOH^o = 2.03 × 10^{-5} mol sites/L	
Ionic strength	Calculated by MINTEQA2	
PCO_2	Calculated by MINTEQA2	
Edge-Site Reactions:	**Log K**	
	Np(V)	U(VI)
Total radionuclide concentration	1×10^{-6} m	1×10^{-6} m
>AlOH^o + H$^+$ ⇌ >AlOH$_2^+$	8.33[b]	8.33[b]
>AlOH^o ⇌ >AlO$^-$ + H$^+$	-9.73[b]	-9.73[b]
>SiOH^o ⇌ >SiO$^-$ + H$^+$	-7.20[b]	-7.20[b]
>AlOH^o + NpO$_2^+$ + H$_2$O ⇌ >AlO-NpO$_2$(OH)$^-$ + 2H$^+$	-13.79[c]	—
>SiOH^o + NpO$_2^+$ ⇌ >SiOH-NpO$_2^+$	4.05[c]	—
>AlOH^o + UO$_2^{2+}$ ⇌ >AlO-UO$_2^+$ + H$^+$	—	2.70[d]
>SiOH^o + UO$_2^{2+}$ ⇌ >SiO-UO$_2^+$ + H$^+$	—	2.60[d]
>AlOH^o + 3UO$_2^{2+}$ + 5H$_2$O ⇌ >AlO-(UO$_2$)$_3$(OH)$_5^o$ + 6H$^+$	—	-14.95[d]
>SiOH^o + 3UO$_2^{2+}$ + 5H$_2$O ⇌ >SiO-(UO$_2$)$_3$(OH)$_5^o$ + 6H$^+$	—	-15.29[d]

[a]Effective edge site surface area assume to be 10 percent of total N_2-BET surface area (97 m^2/g) (Pabalan et al., 1998).
[b]Acidity constants for am-SiO_2 and α-Al_2O_3 from Turner and Sassman (1996).
[c]Np(V)-montmorillonite binding constants from Turner et al. (1998).
[d]U(VI)-montmorillonite binding constants from Pabalan and Turner (1997).

With regard to sorption, only surface complexation reactions are considered; the slightly acid to alkaline pH solutions in the regional groundwater system are above the pH range for likely ion exchange for actinides, even at low ionic strengths (Pabalan and Turner, 1997; Turner et al., 1998). An M/V ratio of 1 g/L is assumed due to a lack of information on effective M/V ratios in the YM fractures. Modeling over a wide range in M/V ratios (Turner, 1995) suggests that, above a threshold value, there is an overabundance of sorption sites relative to radionuclide concentration and further increases in M/V have relatively little effect

on the predicted sorption maximum. For this reason, the actual value chosen for M/V may be relatively insignificant as long as the selected value is above this threshold.

4.2.3 Diffuse-Layer Model—Modeling Results

4.2.3.1 Np(V)-Montmorillonite Sorption

Given the assumptions listed earlier predicted Np(V) sorption on montmorillonite, normalized to an effective surface area of 9.7 m^2/g (Turner et al., 1998) and expressed in terms of $K_{A'}$ (mL/m^2), is shown in figure 4-1. The distribution is roughly log-normal, with a mean of about $10^{0.86} = 7.2$ mL/m^2 (table 4-2). For an effective surface area of 9.7 m^2/g (Pabalan and Turner, 1997; Turner et al., 1998), this mean $K_{A'}$ corresponds to a mean K_D of about 70 mL/g. The calculated range in K_D (and $K_{A'}$) is greater than five orders of magnitude, from a minimum K_D of 5×10^{-3} mL/g to a maximum of almost 940 mL/g. Plotting K_D against measured pH and C_T shows the effect of system chemistry on sorption. The predicted pH-dependence is very similar to controlled laboratory experiments that show a sharp increase in sorption over a narrow pH range (figure 4-2). Predicted sorption also decreases with increasing C_T (figure 4-3), reflecting the effects of neptunyl-carbonate complexation as discussed in section 4.1.

4.2.3.2 U(VI)-Montmorillonite Sorption

The DLM was used to model U(VI)-montmorillonite sorption with the model parameters given in table 4-1. Predicted U(VI) sorption on montmorillonite, normalized to an effective surface area of 9.7 m^2/g (Pabalan and Turner, 1997) and expressed in terms of $K_{A'}$ (mL/m^2), is shown in figure 4-4. Descriptive statistics are included in table 4-3. The distribution is roughly lognormal, with a mean K_D of about 9 mL/g (mean $K_{A'} = 0.9$ mL/m^2). The bulk of the samples exhibit a low K_D of between 1 and 100 mL/g ($0.1 < K_{A'} < 10$ mL/m^2), but the total range in calculated K_D (and $K_{A'}$) is over nine orders of magnitude, indicating the large range in sorption that may occur in fracture groundwater at YM. Plotting K_D against measured pH (figure 4-5) and C_T (figure 4-6) shows the effect of system chemistry on U(VI) sorption. As opposed to the positive correlation shown in figure 4-2, U(VI)-montmorillonite sorption shows a decrease in sorption with increasing pH for the YM groundwaters. The predicted pH-dependence (figure 4-5) is very similar to controlled laboratory experimental results (Pabalan and Turner, 1997) that show a sharp decrease in sorption over a narrow pH range in the presence of aqueous carbonate. The negative correlation between U(VI) sorption and C_T is also shown in figure 4-6. Those waters that have the lowest carbonate concentrations are predicted to exhibit the highest U(VI) sorption. This sorption behavior is consistent with the effects of uranyl-carbonate complexation as discussed in section 4.1.

4.2.4 Incorporation of Predictive Distributions in Performance Assessment

The predicted Np(V) and U(VI) sorption behavior presented in figures 4-1 and 4-4 represents a means of constraining the development of PA PDFs. Descriptive statistics such as those given in tables 4-2 and 4-3 represent the type of information that can be directly incorporated into PA models, including distribution type, mean values, upper and lower limits, and standard deviations. For Np(V)- and U(VI)-montmorillonite sorption, the $K_{A'}$ (mL/m^2) distribution can be expressed in terms of K_D (mL/g) by multiplying $K_{A'}$ by the effective surface area of 9.7 m^2/g, a constant (Bertetti et al., 1998; Pabalan et al., 1998). For this reason, although the magnitude of the values, is different, the distribution type and descriptive statistics such as standard deviation, sample variance and skewness are the same for the two sorption parameters (e.g., compare columns two and three in tables 4-2 and 4-3). As demonstrated in Bertetti et al. (1998) and Pabalan et al. (1998), Np(V) and U(VI) sorption on aluminosilicate minerals exhibit pH-

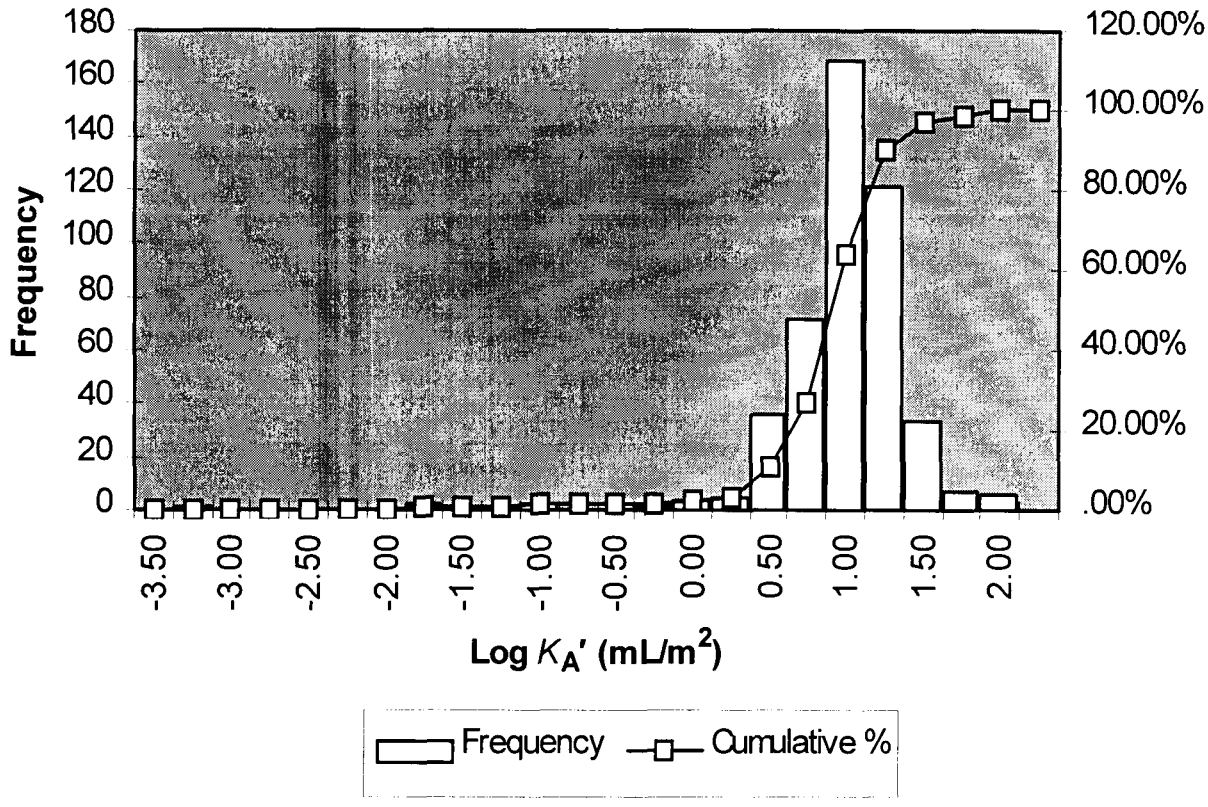

Figure 4-1. Distribution of the calculated Np(V)-montmorillonite sorption coefficient ($K_{A'}$ in mL/m^2) normalized to an effective surface area of 9.7 m^2 (Turner et al., 1998). Calculated with MINTEQA2 (Allison et al., 1991) using a diffuse-layer surface complexation model with parameters given in table 4-1. Water chemistries are for saturated zone regional groundwaters (data from Perfect et al., 1995; see text for details).

dependent behavior that is largely independent of mineral type. The amount of radionuclide sorbed is, instead, mainly a function of surface area. This suggests that the distributions developed in figures 4-1 and 4-4 for sorption on montmorillonite are valid for other aluminosilicate and silicate minerals.

The magnitude of K_D for PA transport calculations can therefore be determined for a given mineral by multiplying the $K_{A'}$ distribution in figure 4-1 (or figure 4-4) by the effective surface area for that mineral. For example, for quartz, the effective surface area is typically small [A′ = 0.03 m^2/g (Bertetti et al., 1998)]. Assuming that the distribution shown in figure 4-1 is valid for Np(V)-quartz sorption, the mean $K_{D,Qz} = K_{A'} \times A' = (7.2\ mL/m^2) \times (0.03\ m^2/g) = 0.2$ mL/g. This value compares well to the low values ($K_{D,Qz} < 1$ mL/g) reported for Np(V) batch sorption studies with crushed tuff and J-13 well water (Triay et al., 1996a). In adapting this approach for PA models of fracture sorption, it may be possible to use as a sampled parameter a form of A′ that represents effective mineral surface area and wetted fracture surface area.

The application of a calibrated sorption model for other radionuclides such as U(VI), Np(V), Pu(V), and Pu(IV) also offers a means of correlating through chemistry the dependence of different radionuclide K_D distributions that is missing in the current Total Performance Assessment code (Wescott et al., 1995). For example, calculating a distribution for U(VI)-montmorillonite sorption for the same set of water analyses used to generate figure 4-1 can provide a direct means of testing the correlation between Np(V) and U(VI)

Table 4-2. Descriptive statistics of predicted Np(V)-montmorillonite sorption for groundwater chemistries reported in Perfect et al. (1995) derived using the Diffuse-Layer Model with model parameters given in table 4-1.

Np(V)-Montmorillonite	Log K_D (mL/g)	Log K_A' (mL/m^2)
Mean	1.85	0.86
Standard Error	0.02	0.02
Median	1.89	0.90
Mode	2.07	1.09
Standard Deviation	0.44	0.44
Kurtosis	24.53	24.53
Skewness	-3.45	-3.45
Range	5.24	5.24
Minimum	-2.27	-3.26
Maximum	2.96	1.97
Count	460	460

sorption that takes into account at least some of the observed ranges in ambient chemistry. Correlation between two datasets (ρ) can be defined as

$$\rho = \frac{\mathbf{Cov(x,y)}}{\sigma_x \sigma_y} \tag{4-3}$$

where:

$$\mathbf{Cov(x,y)} = \frac{1}{n} \sum_{j=1}^{n} (x_j - \mu_x)(y_j - \mu_y) \tag{4-4}$$

and $\sigma_{x,y}$ and $\mu_{x,y}$ represent the standard deviation and mean for each dataset, respectively. For Np(V) and U(VI) sorption on montmorillonite, the calculated correlation is about 0.5, indicating a positive correlation between calculated sorption coefficient PDFs (figure 4-7) due to the effects of the variability observed in the groundwater chemistry near YM. If, as assumed, the observed groundwater chemistry bounds the water chemistry in the fractures at YM, then this correlation should also hold true for sorption in the fractures. It is important to remember that these sorption models were calibrated in end-member experimental systems (Pabalan and Turner, 1997; Turner et al., 1998), and the correlation does not take into account possible competition among radionuclides for available sorption sites.

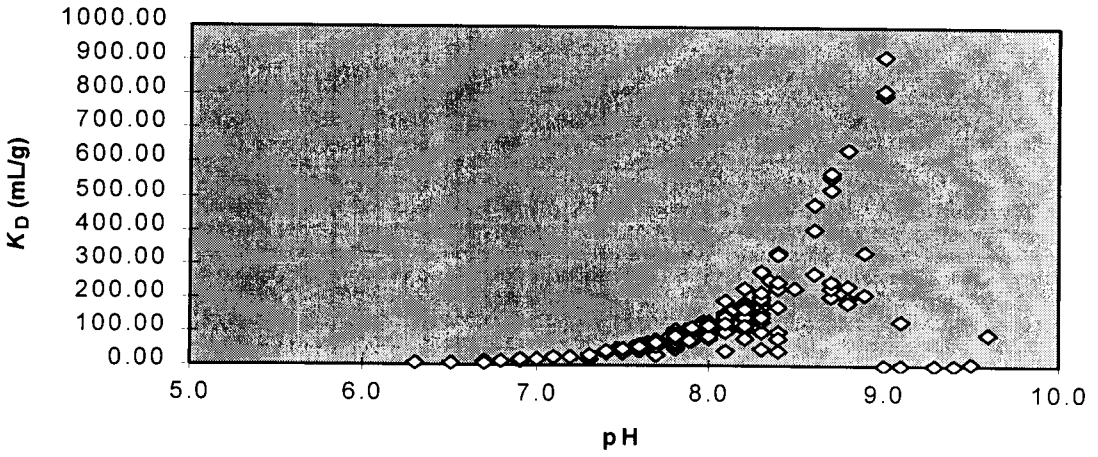

Figure 4-2. Calculated Np(V)-montmorillonite sorption coefficient (K_D in mL/g) as a function of groundwater pH. Calculated with MINTEQA2 (Allison et al., 1991) using a diffuse-layer surface complexation model with parameters given in table 4-1. Water chemistries are for saturated zone regional groundwaters (data from Perfect et al., 1995; see text for details).

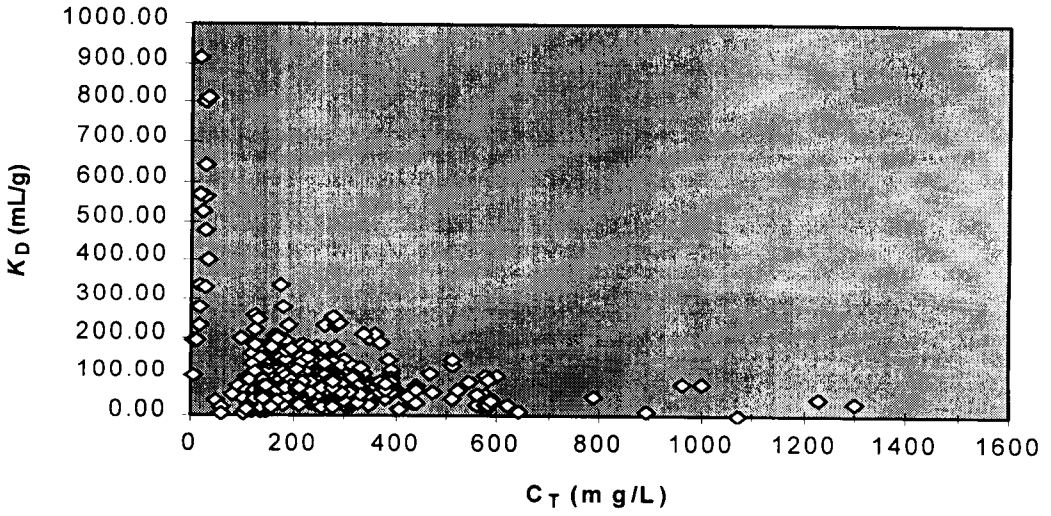

Figure 4-3. Calculated Np(V)montmorillonite sorption coefficient (K_D in mL/g) as a function of groundwater C_T (in mg/L), calculated with MINTEQA2 (Allison et al., 1991) using a diffuse-layer surface complexation model with parameters given in table 4-1. Water chemistries are for saturated zone regional groundwaters (data from Perfect et al., 1995; see text for details). Values calculated for CT> 1,600 mg/L are omitted for clarity.

Table 4-3. Descriptive statistics of predicted U(VI)-montmorillonite sorption for groundwater chemistries reported in Perfect et al. (1995), derived using the Diffuse-Layer Model parameters given in table 4-1.

U(V)-Montmorillonite	Log K_D (mL/g)	Log $K_{A'}$ (mL/m^2)
Mean	0.96	-0.03
Standard Error	0.05	0.05
Median	0.99	0.002
Mode	0.83	-0.16
Standard Deviation	0.98	0.98
Kurtosis	12.93	12.93
Skewness	-2.32	-2.32
Range	9.41	9.41
Minimum	-5.85	-6.84
Maximum	3.56	2.57
Count	460	460

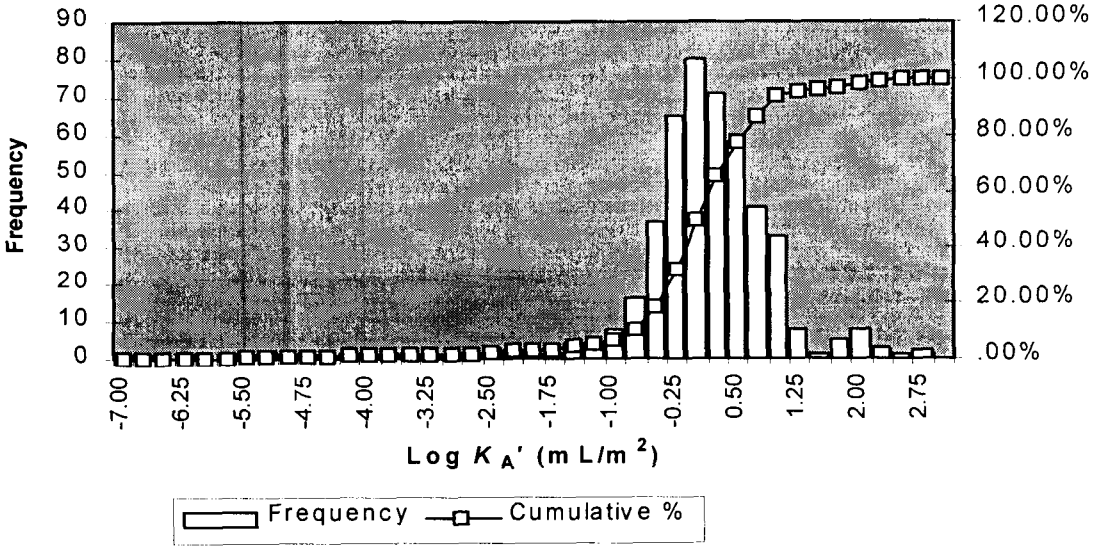

Figure 4-4. Distribution of the calculated U(VI)-montmorillonite sorption coefficient ($K_{A'}$ in mL/m^2) normalized to an effective surface area of 9.7 m^2/g (Pabalan and Turner, 1997). Calculated with MINTEQA2 (Allison et al., 1991) using a diffuse-layer surface complexation model with parameters given in table 4-1. Water chemistries are for saturated zone regional groundwaters (data from Perfect et al., 1995; see text for details).

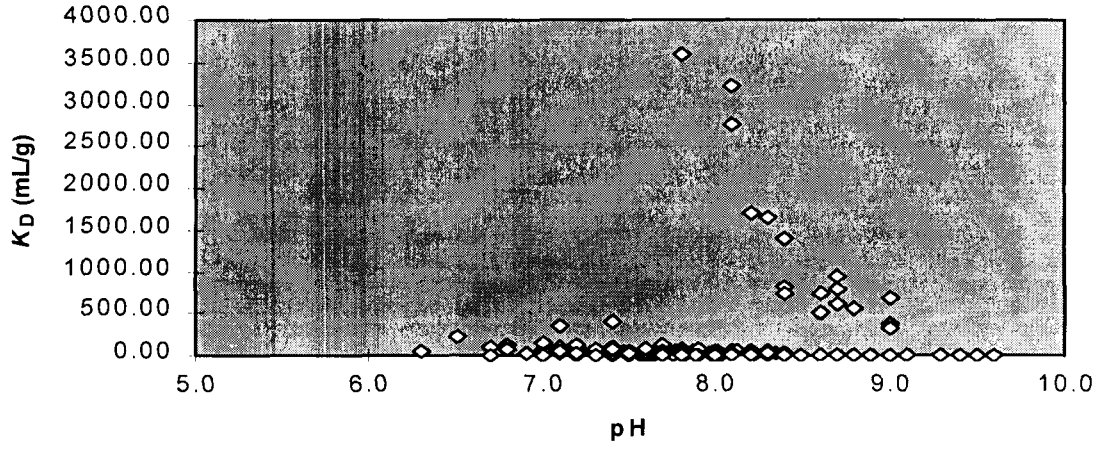

Figure 4-5. Calculated U(VI)-montmorillonite sorption coefficient (K_D in mL/g) as a function of groundwater pH. Calculated with MINTEQA2 (Allison et al., 1991) using a diffuse-layer surface complexation model with parameters given in table 4-1. Water chemistries are for saturated zone regional groundwater (date from Perfect et al., 1995; see text for details

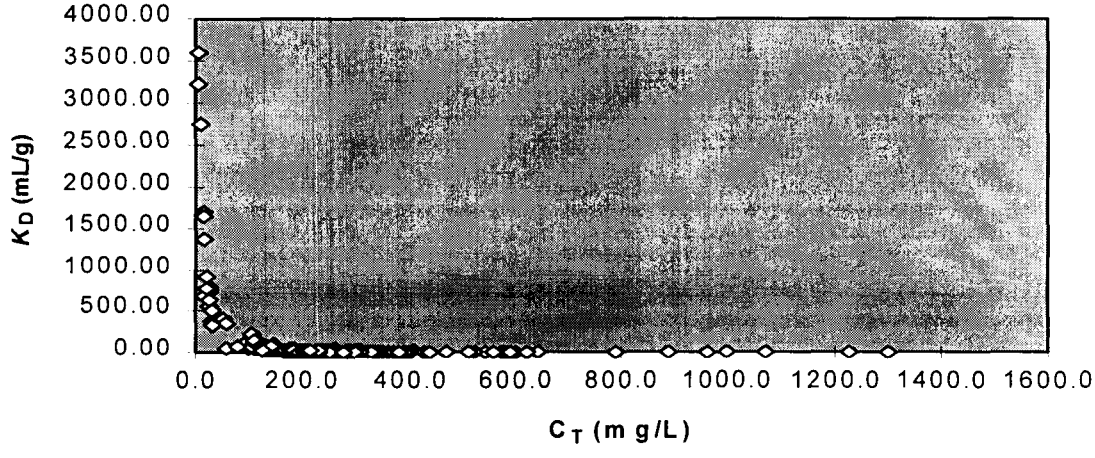

Figure 4-6. Calculated U(VI)-montmorillonite sorption coefficient (K_D in mL/g) as a function of groundwater C_T (in mg/L). Calculated with MINTEQA2 (Allison et al., 1991) using diffuse-layer surface complexation model with parameters given in table 4-1. Water chemistries are for saturated zone regional groundwaters (data from Perfect et al., 1995; see text for details). Values calculated for CT > 1,600 mg/L are omitted for clarity.

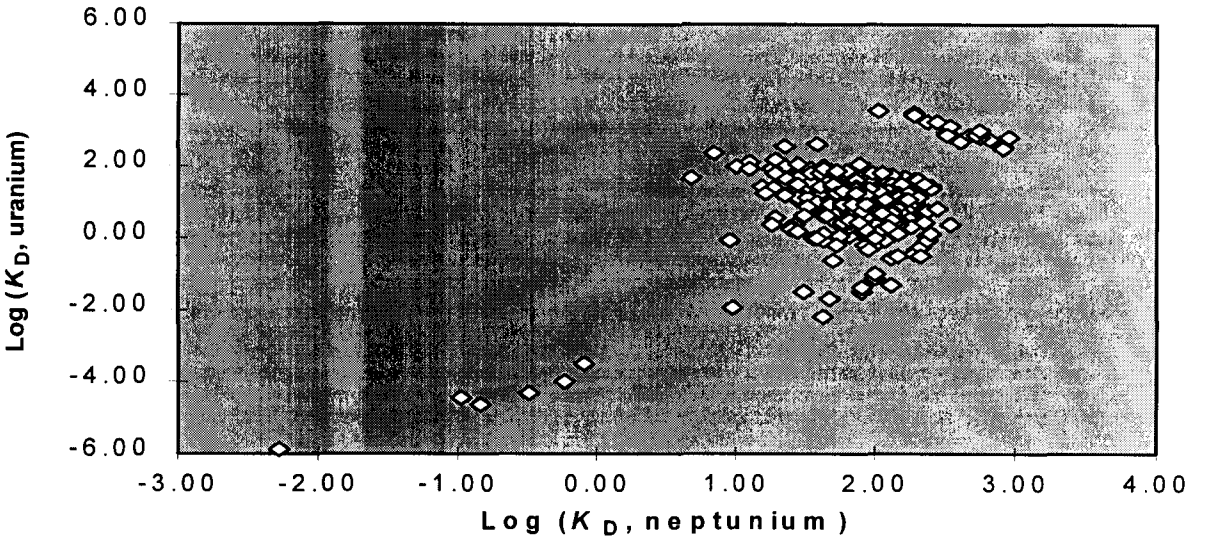

Figure 4-7. Corresponding Np(V)- and U(VI)-montmorillonite sorption coefficients (K_D in mL/g) calculated with MINTEQA2 (Allison et al., 1991) using a diffuse-layer surface complexation model with parameters given in table 4-1. Water chemistries are for saturated zone regional groundwaters (data from Perfect et al., 1995; see text for details).

5 SUMMARY AND CONCLUSIONS

Identifying and evaluating processes affecting RT through fractures has been identified as a subissue in the RT KTI (Nuclear Regulatory Commission, 1998). Certain geochemical processes can both retard RT, delaying arrival times at the critical group location(s), and reduce radionuclide concentrations at the point of exposure. An understanding of geochemical processes that influence RT may be used to compensate for uncertainties in hydrologic models of the YM system (Simmons et al., 1995). Not knowing the degree to which these geochemical processes are affected by changes in system chemistry/hydrology makes it difficult to reasonably bound RT. Regional groundwater chemistry is available in the compilation of Perfect et al. (1995). Screening and culling of these data provided a relatively large set of consistent and complete hydrochemical analyses suitable for geochemical modeling of RT processes. Analyses of measured and derived properties of these groundwaters were used to place limits that are useful to RT calculations for PA.

Ideally, mechanistic sorption models such as surface complexation models would be directly incorporated into reactive transport codes. While hydrogeochemical transport codes may be used to examine particular aspects of reactive transport, the additional computational burden that results from coupling equations for geochemistry and fluid flow may be excessive for the purposes of PA. This is even more important for stochastic approaches that rely on sampling techniques and many realizations to generate CCDFs and population statistics. It may be possible to use the DLM "off-line" to support K_D selection and to assess the effect of critical parameters such as pH and C_T for site-specific conditions.

There are two methods for this type of indirect incorporation of geochemical sorption models into PA. The approach that perhaps more readily is incorporated into current PA codes involves using existing site-specific information on the physical/chemical system at YM with geochemical sorption models to provide realistic constraints on the type and statistical parameters defining the PDFs that describe sorption in PA. This method has been applied here using the compilation of Perfect et al. (1995) to represent the likely variations in regional groundwater chemistry in fractures in the vicinity of YM, and the DLM parameters developed in Pabalan and Turner (1997) and Turner et al. (1998). For Np(V) and U(VI) sorption on montmorillonite, this approach suggests that log-normal distributions of sorption coefficients are appropriate. Both Np(V) and U(VI) are weakly sorbed under the observed groundwater conditions, but total ranges in sorption parameters (K_D or $K_{A'}$) of greater than five [Np(V)] and nine [U(VI)] orders of magnitude were predicted. It is important to remember that the models used here assume that surface complexation is the only mechanism operating to retard radionuclide migration. Other mechanisms such as precipitation/dissolution, ion exchange, and matrix diffusion are not included in this analysis. These sorption models were also calibrated against end-member experimental data, and the effects of competition for available sites by two or more ions are not explicitly considered. Finally, a site concentration was assumed for this system (table 4-1). Significant uncertainty remains in defining the effective fracture surface area available for radionuclide sorption. Values assumed for an effective fracture surface area may have a significant effect if they are small enough that the total site concentration is below a threshold value (Turner, 1995). Above this threshold, the effects of other geochemical parameters may exert more control on sorption, although additional modeling is necessary to constrain this threshold for a given fracture system.

When calibrated for a given radionuclide-mineral system, the DLM approach can be used to define a $K_{A'}$ distribution as a function of key geochemical parameters for site-specific conditions. Because sorption behavior is similar for aluminosilicate minerals (Bertetti et al., 1998; Pabalan et al., 1998), the effective surface area of a given mineral can be used as a scaling factor to convert $K_{A'}$ (mL/m^2) to K_D (mL/g) that can be directly incorporated into PA transport models. Another means of using the DLM approach to constraint

sorption for PA is to apply the model to a wide range of conditions to develop a sorption response surface as a function of key geochemical parameters. Unlike K_D, which is a derived value, geochemical parameters such as pH and C_T are properties of the physical-chemical system that either can be measured or assigned bounding limits. The sorbed and aqueous concentrations calculated using the DLM can be used to develop a range in K_A, (and therefore K_D) values predicted as a function of these variables. One of the most difficult aspects of this type of approach, however, is in determining the appropriate values for model parameters in the natural groundwater system at YM. While geochemical models can be used to limit likely pH and PCO_2 conditions, significant uncertainty remains in determining the effective solid concentration that is "seen" by groundwater containing dissolved radionuclides. As discussed above, detailed knowledge of the M/V ratios may not be critical above a threshold value, but could be significant in considering the effects of sorption in systems with trace amounts of sorptive minerals. With a response surface as a function of geochemical parameters, geochemical variables could be sampled over likely ranges, and the associated K_D used in PA transport calculations. The ranges in these variables could be selected from probability distribution functions based on analysis of the current ambient system. While this is not an explicit incorporation of geochemistry in the transport calculations, it does provide a step towards a more theoretical basis for sorption modeling in PA, and future work will focus on this approach.

6 REFERENCES

Allison, J.D., D.S. Brown, and K.J. Novo-Gradac. 1991. *MINTEQA2/PRODEFA2. A Geochemical Assessment Model for Environmental Systems: Version 3.0 User's Manual.* EPA/600/3-91/021. Athens, GA: Environmental Protection Agency.

Barton, C.C., E. Larsen, W.R. Page, and T.M. Howard. 1993. *Characterizing Fractured Rock for Fluid-flow, Geomechanical, and Paleostress Modelling: Methods and Preliminary Results from Yucca Mountain, Nevada.* USGS-OFR-93-269. Denver, CO: U.S. Geological Survey.

Bertetti, F.P., R.T. Pabalan, and M.G. Almendarez. 1998. Studies of neptunium^{V} sorption on quartz, clinoptilolite, montmorillonite, andα-alumina. E.A. Jenne. ed. *Adsorption of Metals by Geomedia.* New York, NY: Adademic Press, Inc.: 131–148.

Bish, D.L., and J.L. Aronson. 1993. Paleogeothermal and paleohydrologic conditions in silicic tuff from Yucca Mountain, Nevada. *Clays and Clay Minerals* 41: 148–161.

Bish, D.L., J.W. Carey, B.A. Carlos, S.J. Chipera, G.D. Guthrie, Jr., S.S. Levy, D.T. Vaniman, and G. WoldeGabriel. 1996. *Summary and Synthesis Report on Mineralogy and Petrology Studies for the Yucca Mountain Site Characterization Project.* WBS Element 1.2.3.2.1.1 and 1.2.2.2.1.2. Los Alamos, NM: Los Alamos National Laboratory.

Buddemeier, R.W., and J.R. Hunt. 1988. Transport of colloidal contaminants in groundwater: Radionuclide migration at the Nevada Test Site. *Applied Geochemistry* 3: 535–548.

Carlos, B.A. 1985. *Minerals in Fractures of the Unsaturated Zone from Drill Core USW G-4, Yucca Mountain, Nye County, Nevada.* LA-10415-MS. Los Alamos, NM: Los Alamos National Laboratory.

Carlos, B.A. 1987. *Minerals in Fractures of the Saturated Zone from Drill Core USW G-4, Yucca Mountain, Nye County, Nevada.* LA-10927-MS. Los Alamos, NM: Los Alamos National Laboratory.

Carlos, B.A. 1989. *Fracture-Coating Minerals in the Topopah Spring Member and Upper Tuff of Calico Hills from Drill Hole J-13.* LA-11504-MS. Los Alamos, NM: Los Alamos National Laboratory.

Carlos, B.A., D.L. Bish, and S.J. Chipera. 1991. Fracture-lining minerals in the lower Topopah Spring tuff at Yucca Mountain. *Proceedings of the Second International Conference on High Level Radioactive Waste Management.* La Grange Park, IL: American Nuclear Society: 486–493.

Carlos, B.A., S.J. Chipera, D.L. Bish, and S.J. Craven. 1993. Fracture-lining manganese oxide minerals in silicic tuff, Yucca Mountain, Nevada. *Chemical Geology* 107: 47–69.

Carlos, B.A., D.L. Bish, and S.J. Chipera. 1995. Calcite and zeolite fracture coatings in Topopah Spring Tuff along Drill Hole Wash, Yucca Mountain, Nevada. *Proceedings of the Sixth International Conference on High Level Radioactive Waste Management.* La Grange Park, IL: American Nuclear Society: 100–102.

Davis, J.A., and J.O. Leckie. 1978. Surface ionization and complexation at the oxide/water interface 2. Surface properties of amorphous iron oxyhydroxide and adsorption of metal ions. *Journal of Colloid and Interface Science* 67: 90–107.

Davis, J.A., and D.B. Kent. 1990. Surface complexation modeling in aqueous geochemistry. *Reviews in Mineralogy: Volume 23. Mineral-Water Interface Geochemistry.* M.F. Hochella, Jr., and A.F. White, eds. Washington, DC: Mineralogical Society of America: 177–260.

Degueldre, C. 1997. Groundwater colloid properties and their potential influence on radionuclide transport. *Scientific Basis for Nuclear Waste Management XX.* W.J. Gray and I.R. Triay, eds. Pittsburgh, PA: Materials Research Society: Symposium Proceedings 465: 835–846.

Degueldre, C., R. Grauer, and A. Laube. 1996. Colloid properties in granitic groundwater systems. II: Stability and transport study. *Applied Geochemistry* 11: 697–710.

Dzombak, D.A., and F.M.M. Morel. 1990. *Surface Complexation Modeling: Hydrous Ferric Oxide.* New York: John Wiley and Sons.

Hayes, K.F., G. Redden, W. Ela, and J.O. Leckie. 1991. Surface complexation models: An evaluation of model parameter estimation using FITEQL and oxide mineral titration data. *Journal of Colloid and Interface Science* 142:448–469.

Hitchon, B., and M. Brulotte. 1994. Culling criteria for "standard" formation water analyses. *Applied Geochemistry* 9: 637–645.

Kersting, A.B. and J.L. Thompson. 1997. *Near-field migration of radionuclides in the subsurface at the Nevada Test Site: Evidence for colloid transport of radionuclides through fractured volcanic rock.* UCRL-JC-127977 Abstract. Livermore, CA: Lawrence Livermore National Laboratory.

Murphy, W.M. 1995. Contributions of thermodynamic and mass transport modeling to evaluation of groundwater flow and groundwater travel time at Yucca Mountain, Nevada. *Scientific Basis for Nuclear Waste Management XVIII.* T. Murakami and R.C. Ewing, eds. Pittsburgh, PA: Materials Research Society: Symposium Proceedings 412: 419–426.

Murphy, W.M., and R.T. Pabalan. 1994. *Geochemical Investigations Related to the Yucca Mountain Environment and Potential Nuclear Waste Repository.* NUREG/CR-6288. Washington, DC: Nuclear Regulatory Commission.

National Research Council. 1995. *Technical Bases for Yucca Mountain Standards.* Washington, DC: National Academy Press.

Nuclear Regulatory Commission. 1998. *Issue Resolution Status Report on Radionuclide Transport.* Washington, DC: Nuclear Regulatory Commission.

Pabalan, R.T., and D.R. Turner. 1997. Uranium(6+) sorption on montmorillonite: Experimental and surface complexation modeling study. *Aqueous Geochemistry* 2: 203–226.

Pabalan, R.T., D.R. Turner, F.P. Bertetti, and J.D. Prikryl. 1998. Uranium^{VI} sorption onto selected mineral surfaces. E.A. Jenne. ed. *Adsorption of Metals by Geomedia.* New York, NY: Adademic Press, Inc.: 99–130.

Perfect, D.L., C.C. Faunt, W.C. Steinkampf, and A.K. Turner. 1995. *Hydrochemical Data Base for the Death Valley Region, California and Nevada.* USGS Open-File Report 94-305. Denver, CO: U.S. Geological Survey.

Reimus, P.W., and H.J. Turin. 1997. *Results, Analyses, and Interpretation of Reactive Tracer Tests in the Lower Bullfrog Tuff at the C-Wells, Yucca Mountain, Nevada.* Draft Report. Los Alamos, NM: Los Alamos National Laboratory.

Simmons, A.M., S.T. Nelson, P.L. Cloke, T.R. Crump, C.J. Duffy, W.E. Glassley, Z.E. Peterman, M.D. Siegel, D. Stahl, W.C. Steinkampf, and B.E. Viani. 1995. *The Critical Role of Geochemistry in the Program Approach.* Las Vegas, NV: U.S. Department of Energy.

Smith, D.K. 1997. *A Recent Drilling Program to Investigate Radionuclide Migration at the Nevada Test Site. A Paper Prepared for Submittal to the Fourth International Conference on Methods and Applications of Radioanalytical Chemistry.* UCRL-JC-127013 Preprint. Livermore, CA: Lawrence Livermore National Laboratory.

Snyder, J. 1987. *Map Projections, A Working Manual.* USGS Professional Paper 1395. Washington, DC: U.S. Geological Survey.

Sweetkind, D.S., and S.C. Williams-Stroud. 1996. *Characteristics of Fractures at Yucca Mountain, Nevada: Synthesis report.* Denver, CO: U.S. Geological Survey.

Triay, I.R. 1998. *Colloid Formation and Stability.* Presentation to the DOE/NRC Technical Exchange on Total System Performance Assessment - Viability Assessment, held March 17-19, 1998, in San Antonio, TX. Los Alamos, NM: Los Alamos National Laboratory.

Triay, I.R., C.R. Cotter, M.H. Huddleston, D.D. Leonard, S.C. Weaver, S.J. Chipera, D.L. Bish, A. Meijer, and J.A. Canepa. 1996a. *Batch Sorption Results for Neptunium Transport Through Yucca Mountain Tuffs. Yucca Mountain Site Characterization Program, Milestone 3349.* LA-12961-MS/UC-814. Los Alamos, NM: Los Alamos National Laboratory.

Triay, I.R., A. Meijer, J.L. Conca, K.S. Kung, R.S. Rundberg, and E.A. Strietelmeier. 1996b. *Summary and Synthesis Report on Radionuclide Retardation for the Yucca Mountain Site Characterization Project.* Milestone 3784. Los Alamos, NM: Chemical Science and Technology Division, Los Alamos National Laboratory.

TRW Environmental Safety Systems, Inc. 1995. *Total System Performance—1995: An Evaluation of the Potential Yucca Mountain Repository.* B00000000-01717-22000-00136, Rev. 01. Las Vegas, NV: TRW Environmental Safety Systems, Inc.

Turner, D.R. 1993. *Mechanistic Approaches to Radionuclide Sorption Modeling.* CNWRA 93-019. San Antonio, TX: Center for Nuclear Waste Regulatory Analyses.

Turner, D.R. 1995. *A Uniform Approach to Surface Complexation Modeling of Radionuclide Sorption.* CNWRA 95-001. San Antonio, TX: Center for Nuclear Waste Regulatory Analyses.

Turner, D.R., and S.A. Sassman. 1996. Approaches to sorption modeling for high-level waste performance assessment. *Journal of Contaminant Hydrology* 21: 311–332.

Turner, D.R., R.T. Pabalan, and F.P.Bertetti. 1998. Neptunium(V) sorption on montmorillonite: An experimental and surface complexation modeling study. *Clays and Clay Minerals* (in press).

U.S. Department of Energy. 1996. *Highlights of the U.S. Department of Energy's Updated Waste Containment and Isolation Strategy for the Yucca Mountain Site.* DOE Concurrence Draft presented to the Nuclear Waste Technical Review Board in Denver, CO, July 1996.

U.S. Department of Energy. 1998. *Repository Safety Strategy: U.S. Department of Energy's Strategy to Protect Public Health and Safety After Closure of a Yucca Mountain Repository.* Revision 1. Washington, DC: U.S. Department of Energy, Office of Civilian Radioactive Waste Management.

Vaniman, D.T., D.L. Bish, S.J. Chipera, B.A. Carlos, and G.D. Guthrie. 1996. *Summary and Synthesis Report on Mineralogy and Petrology Studies for the Yucca Mountain Site Characterization Project. Volume 1. Chemistry and Mineralogy of the Transport Environment at Yucca Mountain.* Milestone 3665. U.S. Department of Energy, Earth and Environmental Sciences. Los Alamos National Laboratory: Los Alamos, NM.

Wescott, R.G., M.P. Lee, N.A. Eisenberg, and T.J. McCartin. 1995. *NRC Iterative Performance Assessment Phase 2: Development of Capabilities for Review of a Performance Assessment for a High-Level Waste Repository.* NUREG-1464. Washington, DC: Nuclear Regulatory Commission.

Westall, J.C., and H. Hohl. 1980. A comparison of electrostatic models for the oxide/solution interface. *Advances in Colloid and Interface Science* 12: 265–294.

White, A.F., H.C. Claassen, and L.V. Benson. 1980. *The Effect of Dissolution of Volcanic Glass on the Water Chemistry in a Tuffaceous Aquifer, Rainier Mesa, Nevada.* Water-Supply Paper 1535-Q. Washington, DC: U.S. Geological Survey.

Wilson, M.L., J.H. Gauthier, R.W. Barnard, G.E. Barr, and H.A. Dockery, et. al. 1994. *Total System Performance Assessment for Yucca Mountain - SNL Second Iteration (TSPA-1993).* SAND93-2675. Albuquerque, NM: Sandia National Laboratories.

Yang, I.C., G.W. Rattray, and P. Yu. 1996a. *Interpretation of Chemical and Isotopic Data from Boreholes in the Unsaturated Zone at Yucca Mountain, Nevada.* Water Resources Investigations Report 96-4058. Denver, CO: U.S. Geological Survey.

Yang, I.C., P, Yu, G.W. Rattray, and D.C. Thorstenson. 1996b. *Hydrochemical Investigations and Geochemical Modeling in Characterizing the Unsaturated Zone at Yucca Mountain, Nevada.* Denver, CO: U.S. Geological Survey.